THE AMERICAN JOURNAL OF ANATOMY 190:245–265 (1991)

Renal Morphology of the Hook-Lipped African Rhinoceros, *Diceros bicornis*, Linnaeus

N.S.R. MALUF
Cleveland, Ohio 44107

ABSTRACT **The kidney of *Diceros bicornis* has about 60 lobes, all appearing peripherally. These are separated by interlobar septa, except for small septal defects through which tubules pass. Renal capsule and interlobar septa are fibromuscular and contain small blood vessels. The kidney is about 65% cortex. It contains about 12.5 × 10^6 glomeruli, which form about 7% of the cortical mass and 4.6% of the renal mass. Diameter of a glomerular capsule is about 244 μm, there being no difference in size across the cortex in these adults. The ureter bifurcates into a cephalic and a caudal, fibromuscular, urothelial-lined conduit, into which open about 23 urothelial-lined infundibula. The common large collecting duct, or tubus maximus, of every lobe opens at the apex of its infundibulum. Two tubi may join into one infundibulum. The tubi and their terminal collecting ducts (of Bellini) are part of the inner medulla. Musculature of conduits and infundibula is largely longitudinal. The calyx may be represented by a circular muscle bundle near the apex of every infundibulum. The large intralobar veins are partly adherent to their infundibulum and calyx and receive arcuate veins via valved orifices. Most branches of the renal artery enter via the interlobar septa. Within a septum they branch again and also supply numerous perforators, which thence enter the cortex. Remaining branches of the renal artery enter cortex directly from without. A fibromuscular scaffolding lies deep to arcuate veins where they contact medulla. Where these veins contact cortical tubules; however, their walls become merely endothelium, like the walls of the interlobular veins.**

INTRODUCTION

The prehensile-lipped or "black" rhinoceros, *Diceros bicornis*, was common in tropical and subtropical Africa until recently (Bruce, 1791; Baker, 1868; Gessi, 1892; Alexander, 1908; Barber, 1958; Sidney, 1965). Slaughter, single births after a gestation of 1.5 years (Asdell, 1946), and a hemolytic anemia of obscure etiology in captive individuals (Miller and Boever, 1982; Chaplin et al., 1986; Paglia et al., 1986) threaten it with extinction.

In the Miocene, 15 million years ago, the rhinocerines occurred throughout Eurasia, Africa, and North America (Scott, 1937; Colbert, 1969). They are now restricted to southeastern Asia (three species) and to parts of subsaharan Africa (two species). The kidney of *Rhinoceros indicus*, the major Asiatic species, has been studied by the writer (Maluf, 1987). Owing to the wide geographical barrier between *R. unicornis* and *D. bicornis*, a study of the kidney of the latter was indicated. This was especially so because the kidney of the manatee (Maluf, 1989a) was found to be radically different from that of the dugong (Rapp, 1837; Hill, 1945), an otherwise structurally closely related sirenian. During investigation of the *D. bicornis* kidney, hitherto unreported facts emerged with regard to the arterial supply. These were found to apply also to the kidneys of *R. unicornis* and of the African broad-lipped or "white" rhinoceros, *Ceratotherium simum*.

MATERIAL AND METHODS

Material

The right kidney of *D. bicornis* was obtained from a 12-year-old well nourished female (No. 17983), which had been drowned during the evening by an aggressive male. She was necropsied early the following morning, and the midcoronally cut kidney was preserved in 10% formalin. The left kidney was from a 16-year-old female *D. bicornis* (No. 20317), which died of tuberculous pneumonitis and was necropsied on the day of death. This intact kidney was promptly frozen. After it was thawed gradually in a refrigerator, a pyelogram was obtained, and it was perfused via artery and vein with 10% formalin, divided midcoronally, and preserved in formalin. Both kidneys of this animal were approximately the same size and shape and were without grossly detectable scars.

Histological Sections

Sections 5 μm thick were cut from paraffin-embedded tissue. The stains used were modified Masson's (1929) trichrome (cf. Luna, 1960) and Weigert's (1898) and Verhoeff's (1908) for elastin. With the trichrome, muscle was pink and collagen blue. With the stains for elastin, collagen was very light pink and muscle very light yellow. Thus, in differentiating muscle from collagen, the trichrome and the elastin stains complemented each other.

Received March 5, 1990. Accepted October 3, 1990.

Address reprint requests to N.S.R. Maluf, MSc, PhD, MD, ChM, FRCS, 12500 Edgewater Drive, Cleveland, OH 44107.

Counting of Lobes and Dissection

Emphasis was on careful dissection using fiberoptic illumination and dissecting microscope (×7–30). A pair of fine watchmakers' forceps and straight ophthalmic scissors were indispensable. Measurements were made usually with fine draughtman's dividers provided with a set-screw. The lobes were counted, after stripping superficial fascia, by numbering with green tempera. Figures 1–4 were done with assistance of photographs.

In several instances, the range of linear measurements is given rather than "averages." For example, the width of areolar fascia between renal capsule and pelvic conduit is from 512 to 5,120 μm. The wide range in this instance is due largely to the diameters of blood vessels coursing through this fascia. One can obtain any sort of meaningless "statistical average" depending on the locus of measurement. The same applies to cortical and medullary thicknesses and longitudinal folds of the ureter, which undulate. The width of lumen of an infundibulum varies with distance from the infundibular orifice. A great number of linear measurements were taken from many lobes in arriving at the quoted ranges. Where averages are feasible they are given, e.g., glomeruli, diameter of terminal collecting ducts, etc.

Counting of Glomeruli

Glomerular counts were done as previously (Maluf, 1989a). Blocks of central cortex, 3.62–3.91 g, were weighed to the nearest milligram after being mopped thoroughly on absorbent paper. The blocks were immersed in about 20 ml of 7.4N (27%) HCl in a 50 ml plastic cylinder with screw-cap, kept at room temperature for 2 days, and then transferred to 39°C for several hours. Mild shaking then resulted in a uniform suspension, which was brought precisely to the 40 ml mark with 0.9% NaCl and then refrigerated overnight. An aliquot of 0.010 ml was transferred to a slide by a Gibson pipette (Rainin Instruments, Woburn, MA) and the glomeruli counted. This was repeated 50 times, the container having been shaken immediately before every withdrawal. The glomeruli, including the glomerular capsules, were intact and the tubules were fragmented. This technique is essentially that of Baer et al. (1978).

Volume of Glomerular Capsules

Measurements were taken from the histological sections. Since the capsules were spheroidal, the average of two radii was used to calculate the volume of a sphere. The largest capsules at each of three levels of cortex were chosen because they were considered to have been cut through the meridian. The tubular or vascular pole, or both, was usually evident. Mean capsular diameters measured from thin razor slices of the fixed cortex (237 μm ± 12; n = 13) corresponded with those in the paraffin sections (244 μm ± 13; n = 36). Volume in cubic millimeters was converted into mg by multiplying by 1.060.

Relative Mass of Cortex and Medulla

The coronal half of a kidney was cut transversely into slices about 5 mm thick. Interlobar connective tissue with contained vessels was discarded. Cortex was separated from medulla with curved surgical scissors using a loupe for magnification. The numerous arcuate vessels were the main landmarks in addition to differences in appearance between cortex and medulla. The combined slivers of cortex and, separately, of medulla were mopped thoroughly on absorbent paper and weighed to the nearest milligram.

Maceration

In studies of the medulla, slices about 3mm thick through both cortex and medulla were immersed in 7.4 N HCl only until the tissue became quite soft and could not be grasped. The tissue then was washed carefully with 0.9% NaCl after decanting the HCl. Dissections were done in the saline under the dissecting microscope with fine steel entomological pins (4-0) in holders, as described previously (Maluf, 1989a). Specimens were transferred by pipette to a depression slide for examination and measurement by transmitted light at ×100.

Pyelogram

A pyelogram was obtained by injecting Renografin-76 (Squibb), a solution containing 37% organically bound iodine, through a catheter fitted into the ureter. The kidney was on the cassette directly over the film. The terminal collecting ducts became injected retrogradely, which is common for ducts opening at a tubus maximus.

RESULTS

General Results

The kidneys are C-shaped. The cephalic and caudal poles approximate each other medially (Figs. 1–4). The tough superficial enveloping fascia, not shown in the illustrations, assists in maintaining the C formation while not entirely masking the compact lobation. Fat occurs within this fascia but not deep to the renal capsule. The latter extends between the lobes as interlobar

Abbreviations

A	Arcuate vessels
AA	Arcuate artery
AF	Areolar fascia
AV	Arcuate vein
B	Vascular bundle
C	Cortex
CO	Conduit
CX	Calyx
IF	Infundibulum
ILA	Interlobar artery
ILV	Interlobar vein
IM	Inner medulla
IN_1, IN_2, IN_3	Orifice of primary, secondary, and tertiary infundibula, respectively
INLV	Intralobar vein
OM	Outer medulla
P	Pelvis proper
P_1, P_2	Cephalic and caudal pelvic conduits, respectively
PA	Perforating artery
PR	Projection of arcuate vein
RA	Renal artery
RC	Renal capsule
RV	Renal vein
S	Interlobar septum
TM	Tubus maximus
U	Ureter
V	Large interlobar vein

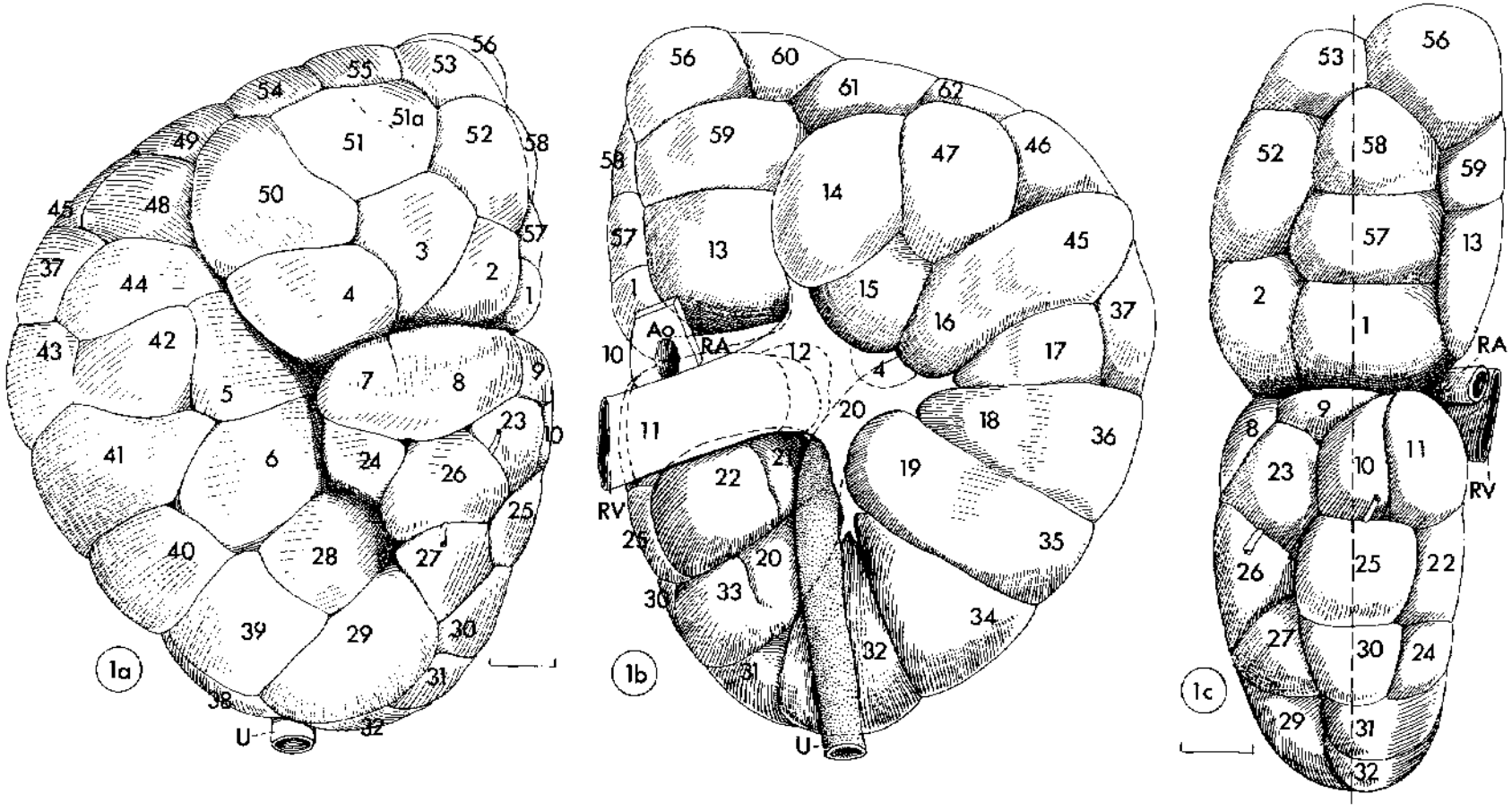

Fig. 1. Left kidney of No. 20317 with the lobes numbered. **a:** Dorsal aspect. Superficial fascia and renal capsule, up to the interlobar sulci, have been removed. There is a deep cleft between cephalic and caudal poles. Bar = 2.5 cm. **b:** Ventral aspect. The deep cleft between cephalic and caudal poles contains contents of the hilum and renal sinus. Ao, Aorta. **c:** Medial aspect. The broken line represents the coronal cut shown in Figure 3. Bar = 2.47 cm.

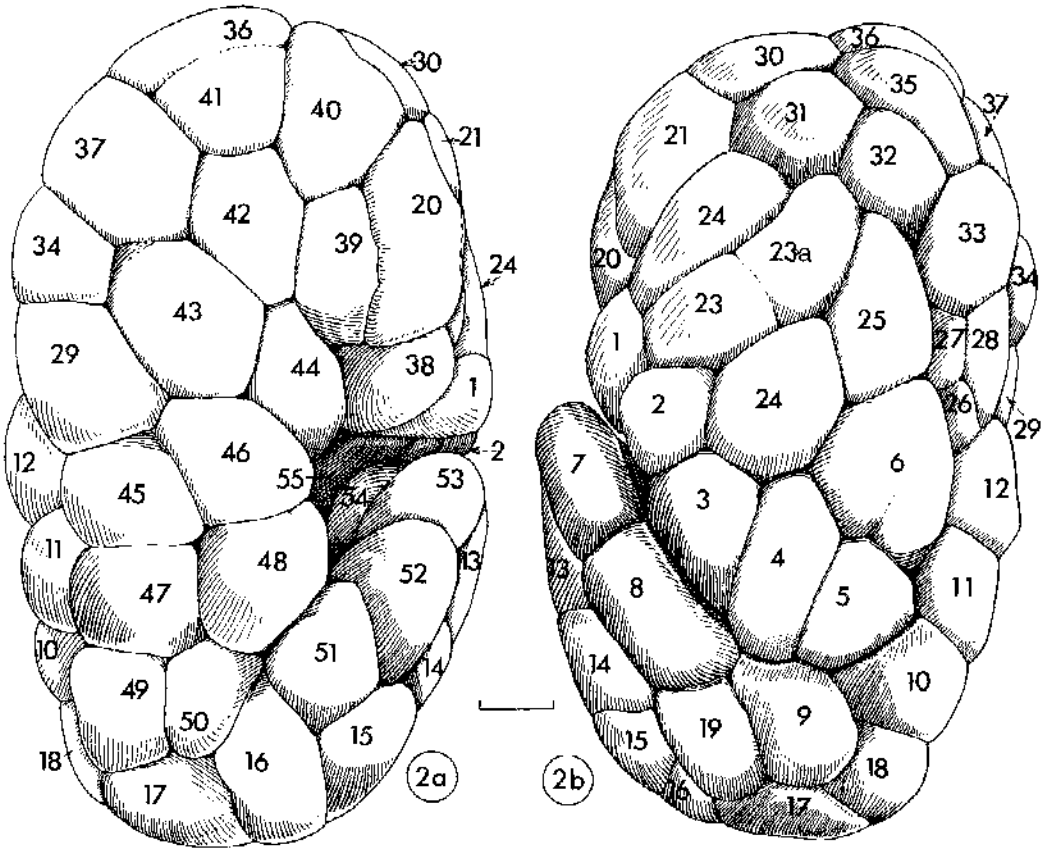

Fig. 2. Right kidney of No. 17983. **a:** Ventral aspect. The hilum and renal sinus are shown in part. Superficial fascia and renal capsule, up to the interlobar sulci, have been removed. Bar = 2.34 cm. **b:** Dorsal aspect. The caudal pole is overlapped by lobes 2 to 5 of the cephalic pole.

septa. All lobes present externally. The renal sinus is part of the renal surface, although it cannot be exposed without prying apart the cephalic and cranial poles. Hence lobes concealed within the renal sinus are considered as presenting externally, e.g., lobes 4, 12, and 20 (Fig. 1b) and lobes 54 and 55 (Fig. 2a).

A midcoronal cut through a kidney shows that the ureter (Figs. 3, 4) bifurcates into a cephalic and a caudal pelvic conduit. This is confirmed by the pyelogram. Furthermore, these coronal cuts indicate that the renal lobation is transverse across the conduits. Transverse lobation can be detected also from the medial aspect (Fig. 1c). Transverse lobation is not striking at the dorsal (Figs. 1a, 2b) or ventral (Figs. 1b, 2a) aspects of the kidney because of developmental crowding, slipping of lobes, and bifurcation of infundibula.

At the surface, lobes ranged between 28 and 73 mm in maximal linear dimension (Table 1). The depth of the lobes was limited by the pelvic conduits (Figs. 3, 4) and ranged between 40 and 56 mm. This was true also for lobes that drained into secondary and tertiary infundibula.

Lobes may be isolated from one another by dissection because of relative sparsity of unifying gaps through the interlobar septa and the existence of moderately sized blood vessels in these septa. Six lobes, prepared from the caudal pole of No. 17983, are shown in Figures 5–10. They are dissimilar in size and shape, tend to have a convex external surface, and are truncated toward the pelvic conduit (Figs. 6, 7). The average mass of a lobe, after excision of interlobar connective tissue and blood vessels, is 29.2 ± 4.8 g. Total number of lobes in the kidney of No. 17983 is 57, which would yield a total lobar mass of 1,670 g. The mass of the entire kidney is 1,855 g, which exceeds this value partly due to the interlobar connective and vascular tissue.

Facetation of the lateral lobar surfaces (Figs. 5–13) is probably due to mutual compression. Three lobes, but not four, come together forming a common interlobar septum (Figs. 1, 2, 21). Interlobar arteries, which traverse through the interlobar septa (see below), do not interfere with the overall compactness of lobation partly because the septa are fused where the arteries do not course.

All terminal collecting ducts (of Bellini) of a lobe open around and into a major collecting duct or tubus maximus. In the rhinoceri, lobes are defined by a separate cortex, medulla, and tubus maximus. A superficial peripheral depression may separate lobes, e.g., lobes 7 and 8 (Fig. 1a) or lobes 16 and 45 (Fig. 1b). In such instances the medullae and their tubi maximi tend to fuse centrally (Fig. 14).

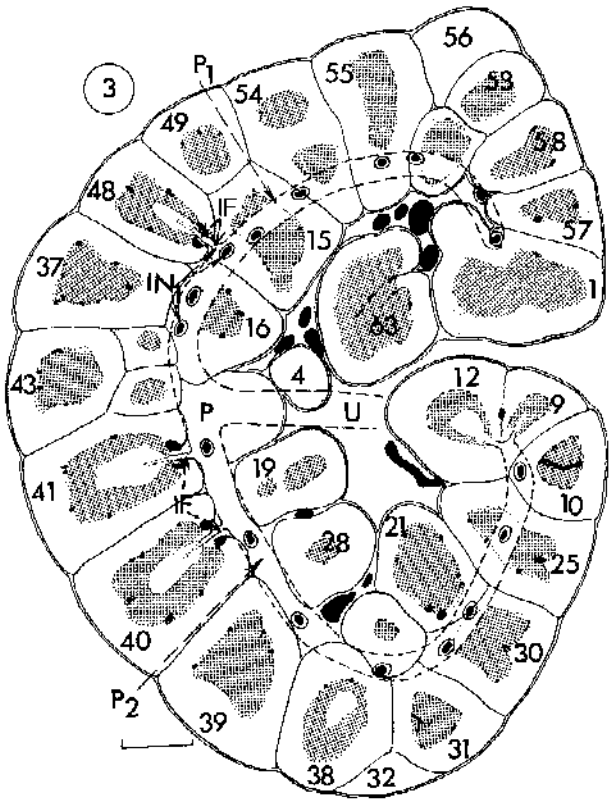

Fig. 3. Dorsal surface of coronal cut through left kidney of No. 20317. Figure 1c shows direction of the cut. The cephalic (P_1) and caudal (P_2) conduits are shown entire after having been exposed by dissection. Orifices to the infundibula are shown as encircled spots. Some orifices are in direct continuity with their infundibula (lobes 48, 41, 40, 12, and 9), and these are not included among the encircled spots. P, pelvis proper. Bar = 2.34 cm.

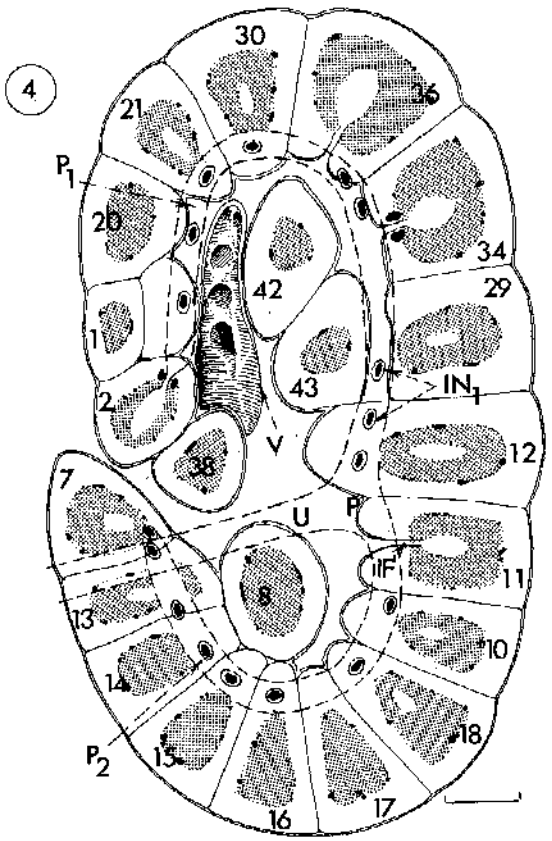

Fig. 4. Ventral surface of coronal cut through right kidney of No. 17983, showing the cephalic and caudal conduits of the pelvis as in Figure 3. Orifices in direct continuity with their infundibula are for lobes 36, 34, 11, and 2. A segment of a large vein in the renal sinus is close to the medial wall of the conduits. Bar 2.35 cm.

TABLE 1. General data for *D. bicornis*

	No. 17983	No. 20317
Age (years)	12	16
Sex	F	F
Kidney	Right	Left
Mass of two kidneys (g)	3,710	5,196
Length of kidney (mm)	270	275
Greatest width of kidney (mm)	145	185
Greatest thickness of kidney (mm)	100	97
No. of lobes/kidney	57	64
Mass of single lobe (g)	29.2 ± 4.8 (n 6)	—
Maximum surface dimension of lobes (mm)	28–73	
Depth of lobes (mm)	40–56	

Ureter and Pelvic Conduits

The ureter at the hilum is about 9 mm in outer diameter (Table 2). It has the following features from lumen to periphery: 1) longitudinal folds of urothelium and tunica propria 500–1,300 μm thick, 2) longitudinal and oblique muscle fibers about 385 μm thick, and 3) circular muscle fibers 1,024 μm thick. The ureter bifurcates near the middle of the kidney into a cephalic and a caudal fibromuscular conduit (Figs. 3, 4). Each conduit has a smooth lining of urothelium and has an internal diameter of about 5 mm. Deep to the urothelium is a narrow layer of collagen, about 84 μm thick, containing fine blood vessels. The rest of the wall, about 525 μm thick, consists of muscle fibers, chiefly longitudinal and oblique, interspersed liberally with collagen bundles. Elastic fibrils occur along the muscle fibers. The conduits are almost equidistant (40–55 mm) from the lateral and medial borders of the kidney (Figs. 3, 4, 11–14). Total length of the conduits is 330 mm (No. 17983) and 380 mm (No. 20317). The cephalic conduit is 190 mm in both individuals. The caudal conduit is 140 mm in No. 17983 and 190 mm in No. 20317. The capacity of the conduits, derived from their length and fairly uniform cross-sectional area, is surprisingly small (Table 2).

The primary orifices of the infundibula, 21 in No. 17983 and 24 in No. 20317, open at all arcs of the conduits. The number of renal lobes per primary infundibulum is 2.71 for No. 17983 and 2.67 for No. 20317;

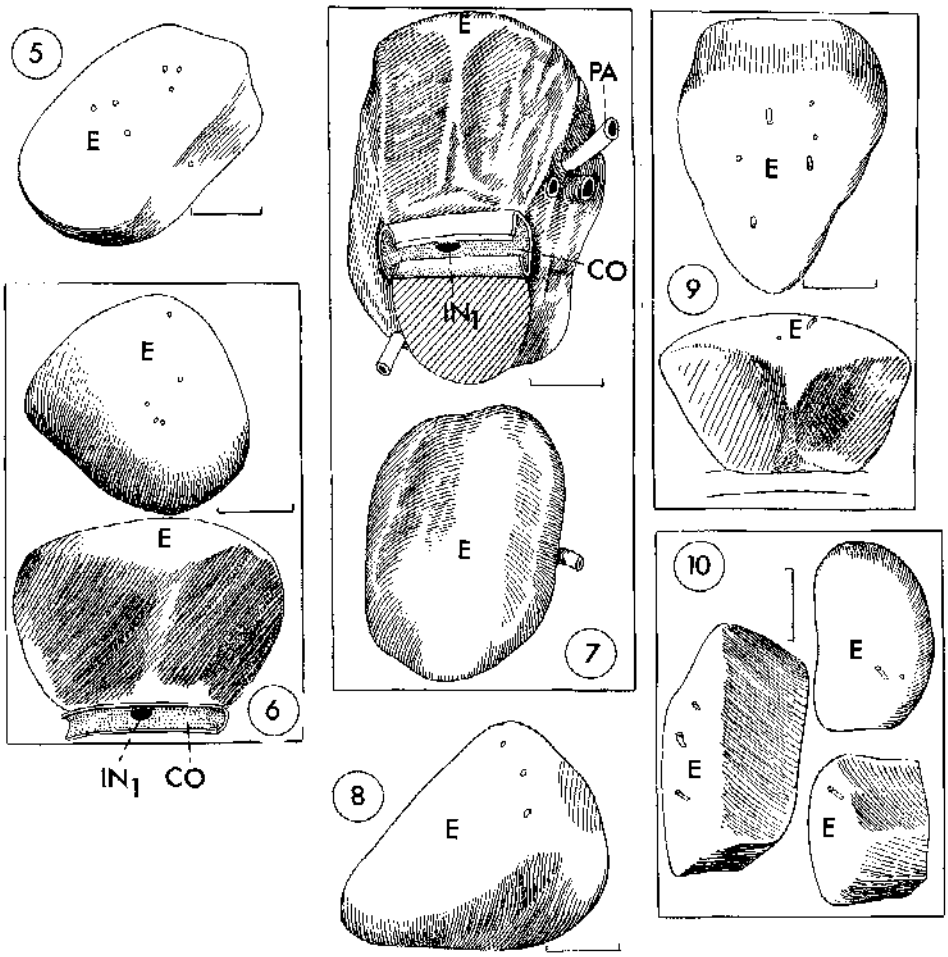

Figs. 5–10. Six lobes dissected whole from the caudal pole of No. 17983. Part of the pelvic conduit is still attached in Figures 6 and 7 along with the orifice of the infundibulum. E, The external surface of each lobe. External perforator vessels are shown as small circles. Bars = 16 mm for Figure 5; 14.6 mm for Figures 6, 10; mm for Figure 8; and 15.4 mm for Figure 9.

TABLE 2. Data for ureter, pelvic conduits, and infundibula of *D. bicornis*

Measurements	No. 17983	No. 20317
Ureter at hilum, outer diameter (mm)	9	
Thickness of circular muscle of ureter (μm)	1,024	
Thickness of longitudinal muscle of ureter (μm)	384	
Thickness of tunica propria of ureter (μm)	500–1,300	
Wall thickness of pelvic conduit (μm)	525	
Length of cephalic conduit (mm)	190	190
Length of caudal conduit (mm)	140	190
Capacity of conduits (cm^3)	6.5	9.0
No. of primary infundibular orifices	21	24
Width of primary infundibular orifice (mm)	2–3	
Length of primary infundibula (mm)	5–20	
Wall thickness of primary infundibulum near orifice (μm)	466 ± 104 (n = 14)	

branching of infundibula explains this disparity. The primary orifices are typically elliptical (1 and 3 mm in diameter). Some, however, are circular and 2–2.5 mm in diameter. The long diameter of the orifices is along the length of the conduits.

Areolar fascia, 512–5,120 μm in width, containing major blood vessels and nerves, intervenes between the conduits, the vessels, and the renal capsule (Fig. 20). This allows contractility of the conduits by avoiding adherence to the renal capsule.

The conduits are probably homologous with a bifurcating pelvis. The infundibula take off from this into

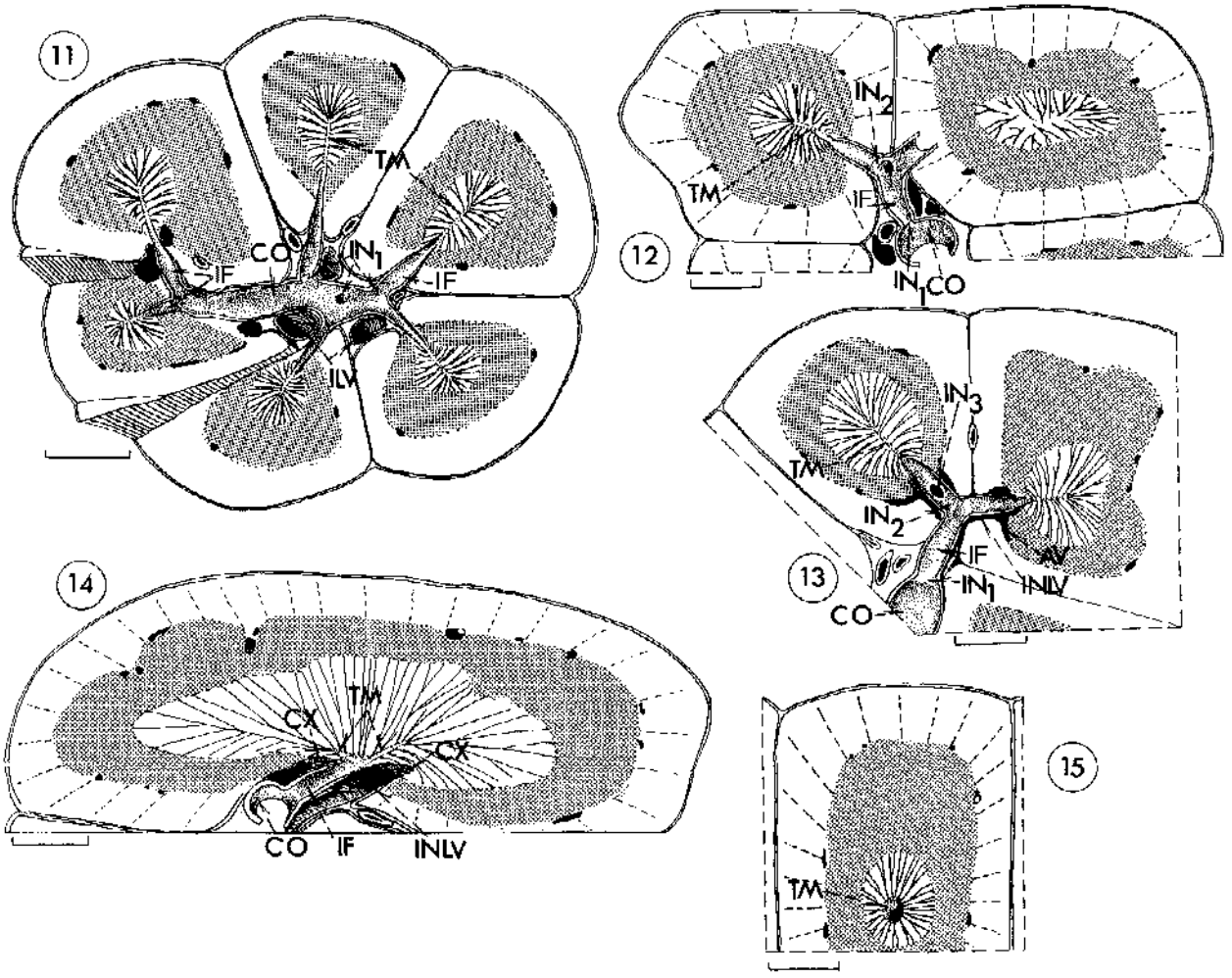

Figs. 11–15. Transverse sections through lobes of No. 20317. Figure 11 is a stepped off-center coronal cut showing branchings of the cephalic conduit. Lobes on the right (lobes 4 and 50 of Fig. 1a) overlap the dorsal surface of the cephalic pole. The interlobar veins run off from the large intralobar veins adjacent to the infundibula (e.g., Fig. 14). Figure 15 is a transverse cut through a tubus maximus. Bars = 20 mm in Figure 1; 9.6 mm in Figures 12, 13; 10 mm in Figure 14; 7 mm in Figure 15.

the lobes and thus express the transverse lobation already noted.

The renal pelvis, or specifically the pelvic conduits of *D. bicornis*, differs from that of *R. unicornis* (Maluf, 1987) in the following ways. 1) *D. bicornis* has no valves at the primary infundibular orifices. A recently acquired neonatal *R. unicornis* (No. 26317) confirms the presence of a membranous valve at every primary orifice. 2) *D. bicornis* has no saccular pelvis; the neonatal *R. unicornis* confirms the existence of a distinct saccular pelvis including the bar at the lateral border of the pelvis (Maluf, 1987). 3) *D. bicornis* has fewer renal lobes per primary infundibular orifice than *R. unicornis:* 2.7 vs. 4.3. Along with this is the markedly greater number of lobes in *R. unicornis* (113 in the above term neonate and 78 in the adult). 4) *D. bicornis* has a smaller conduit capacity than *R. unicornis* because of narrower conduits and absence of a saccular pelvis.

Infundibula

A primary infundibulum extends from every orifice of the pelvic conduits. When such an infundibulum is not fully exposed in the coronal cut (Figs. 3, 4, 11–13), its direction is detected by gentle insertion of a slightly curved dull metal probe, which is cut down upon by a fine scalpel. Secondary and tertiary infundibula are shown in the retrograde pyelogram (Fig. 32) and in the dissections (Figs. 11–14). The primary infundibula are 2–3 mm wide and 5–20 mm long (Table 2). The wall thickness of an infundibulum near its base is almost that of the pelvic conduit: 305–586 μm. Loss of caliber occurs by bifurcation (Fig. 11). The secondary orifices tend to be elliptical (1 and 2 mm), with their long diameters along the length of the primary infundibulum. Some orifices, however, are circular (Figs. 12, 13). Figure 13 includes the orifice of a tertiary infundibulum.

The wall of an infundibulum is lined by urothelium

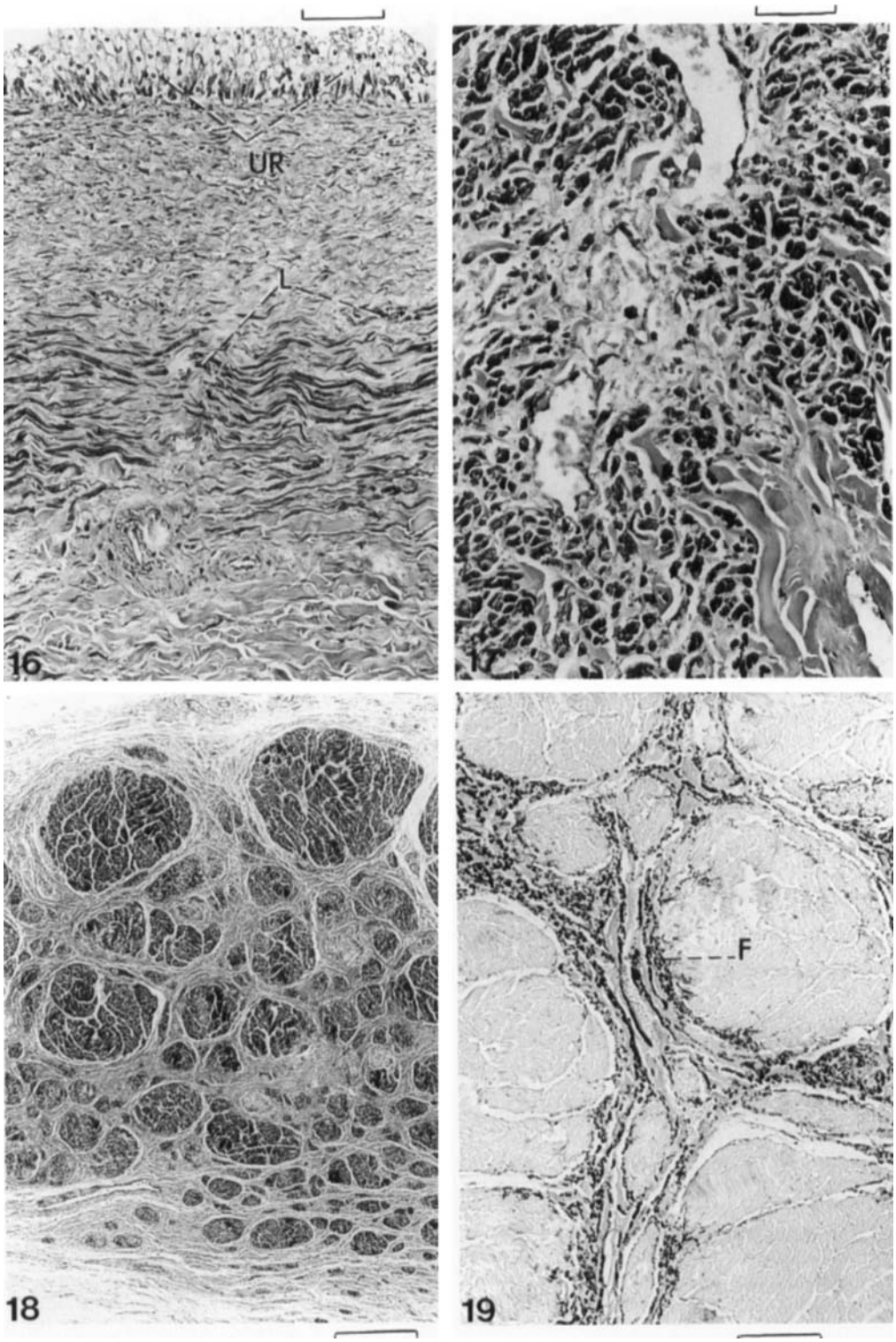

Fig. 16. Wall of shaft of a primary infundibulum. The longitudinal muscles (*L*) are evident. UR, urothelium. No. 17983. Masson's trichrome; Kodak 58 green filter. Bar = 80 μm.

Fig. 17. Cross section through circular muscles of "calyx" of infundibulum of Figure 45. Masson's trichrome; Kodak 58 green filter. Bar = 40 μm.

Fig. 18. Cross section through muscular component of the posterior vena cava at level of right renal vein showing longitudinal muscle bundles. No. 17983. Masson's trichrome; Kodak 58 green filter. Bar = 286 μm.

Fig. 19. Cross section of posterior vena cava at level of Figure 18 showing longitudinal elastic fibers (F) surrounding the muscle bundles. No. 17983. Weigert's elastic. Bar = 167 μm.

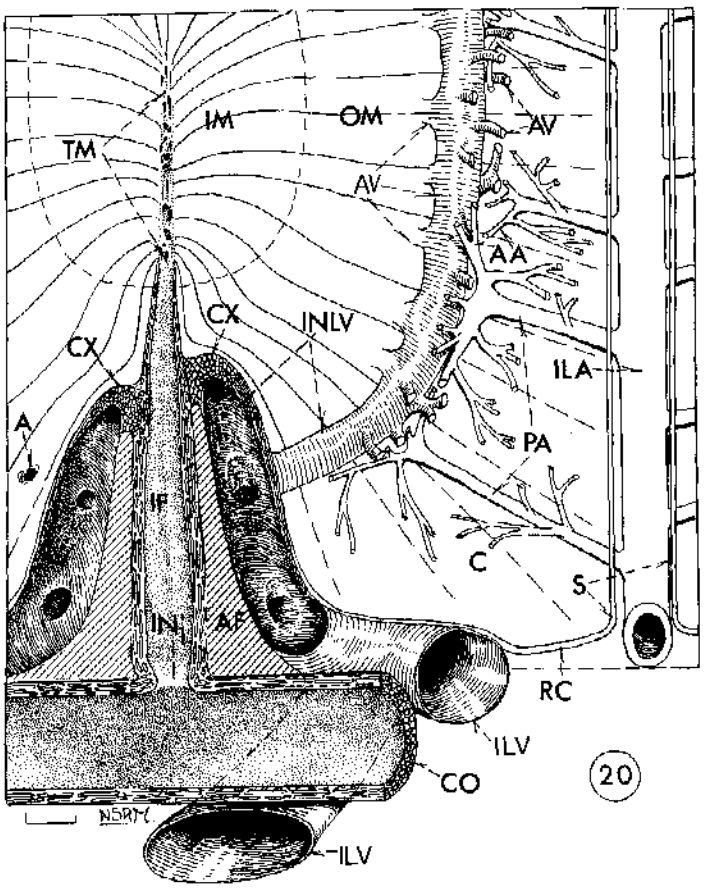

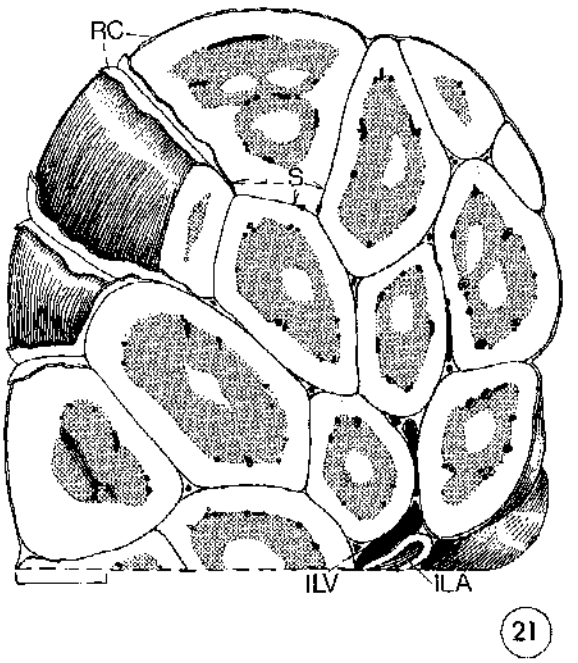

Fig. 20. Semischematic diagram of a longitudinal cut through the base of a renal lobe of D. bicornis with adjacent pelvic conduit and interlobar septum. Bar = 2 mm.

Fig. 21. Superficial coronal cut about 7 mm from surface of cephalic pole of No. 20317. Cortices are white; outer medullae are stippled. Bar = 20 mm.

(Fig. 16) and has longitudinal muscle fibers interspersed with bundles of collagen (Figs. 16, 20). There is usually thickening of the muscularis and narrowing at the infundibular orifice. Near the apex of an infundibulum and close to the tubus maximus there is a conspicuous bundle of circular muscle fibers interspersed with collagen (Figs. 17, 20, 22, 23, 26, 27). This fibromuscular mass or "calyx" does not extend between cortex and medulla as it does in *R. unicornis* (Maluf, 1987). It does, nevertheless, attach to the large intralobar veins (Figs. 14, 20, 22, 23, 26) but not as intimately as in *R. unicornis*. Possible reciprocal function between calyx and intralobar veins has been mentioned in the 1987 paper. Surrounding the infundibulum is a zone of areolar fascia allowing contractility of the infundibulum (Figs. 20, 24). As an infundibulum narrows peripherally it continues to have longitudinal muscle fibers up to where it joins its tubus maximus (Figs. 11–14, 20, 22–24, 26–28).

Cortex

The kidney is about 65% cortex. Interlobar septa separate the cortices of adjacent lobes (Figs. 3, 4, 11–13, 21). The cortex thus is essentially discontinuous, unlike the continuous condition in other mammals with lobar kidneys: manatee, ox, pig, hippopotamus, and man. There are, however, relatively minor gaps in the interlobar septa through which tubules cross. Peripherally the cortex of *D. bicornis* is 7–11 mm thick and 3.5–7 mm at the interlobar septa (Table 3).

The cortex corticis of Toldt (1874) and Heidenhain (1937) is a peripheral layer with tubules but no glomeruli. In adults of *D. bicornis*, this layer is fairly well defined (Fig. 33). It is 218–435 μm thick and may accommodate three to seven tubules in cross section. In the elephant, this layer is virtually nonexistent since glomeruli contact renal capsule in juvenile and adult.

In *D. bicornis* there is no consistent difference in size of glomeruli across the width of the cortex (Table 2, Fig. 33). The diameter of a glomerular capsule is 244 ± 13 μm (n = 36) for both individuals (Table 3), which is larger than the 194 ± 4.5 μm (n = 6) for *R. unicornis* (Maluf, 1987). The kidney of No. 20317 partly compensates for its lower number of glomeruli per gram of cortex and per unit area by being larger than that of No. 17983 (Table 1). Thus the total number of glomeruli is almost equal in the two individuals. Glomerular mass for both, as percent of cortical mass and of renal mass, averages 7.34 and 4.6, respectively (Table 3). This compares with 5.83 and 4.40 for *R. unicornis*

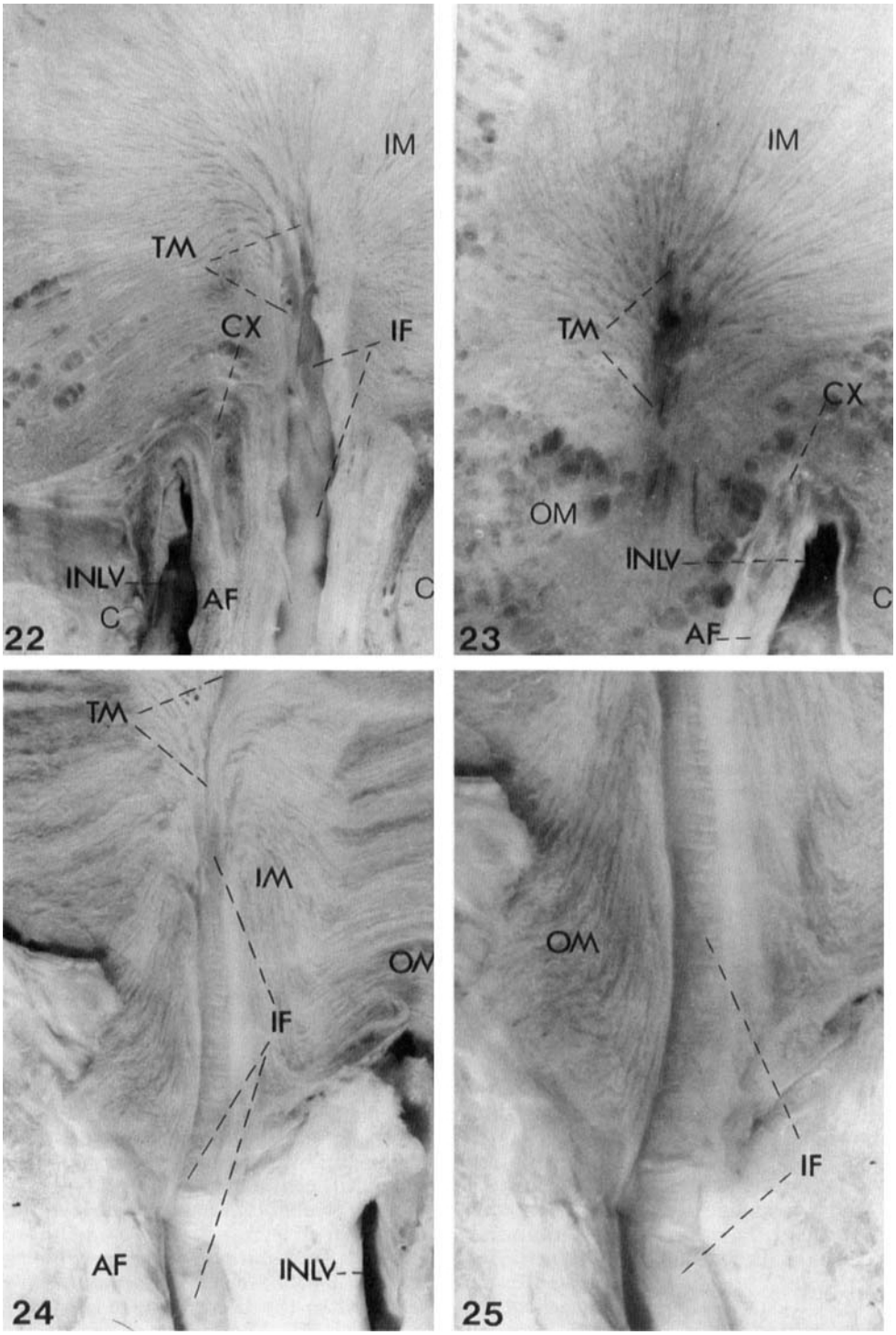

Fig. 22. Photograph of longitudinal cut, immersed in 10% formalin, through a tubus maximus, infundibulum, and intralobar vein. No. 20317. Bar = 4.5 mm.

Fig. 23. Photograph of longitudinal cut, immersed in 10% formalin, through a tubus maximus and intralobar vein. The numerous cysts in the outer medulla are indicative of the hyperparathyroidism in this *D. bicornis* (No. 21362). Bar = 4.5 mm.

Fig. 24. Photograph of longitudinal cut, immersed in 10% formalin, through a tubus maximus, infundibulum, and an intralobar vein. No. 20317. Bar = 4.6 mm.

Fig. 25. Enlargement of part of Figure 34 showing part of infundibulum and outer medulla. Bar = 5.5 mm.

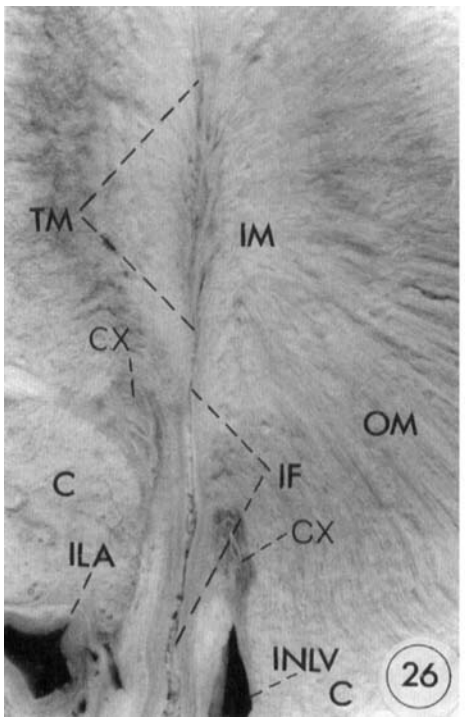

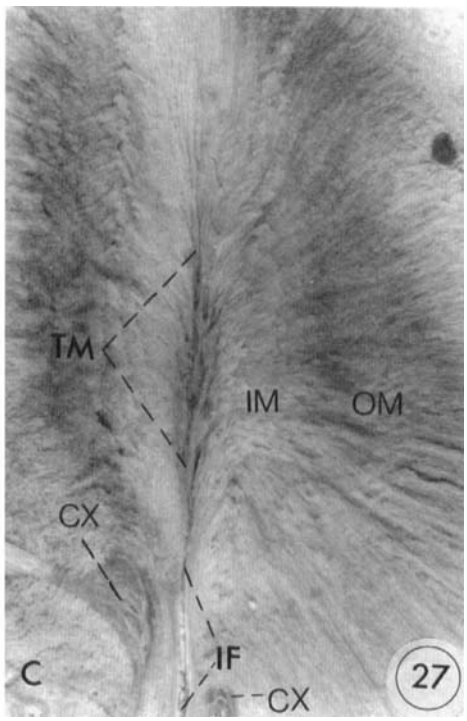

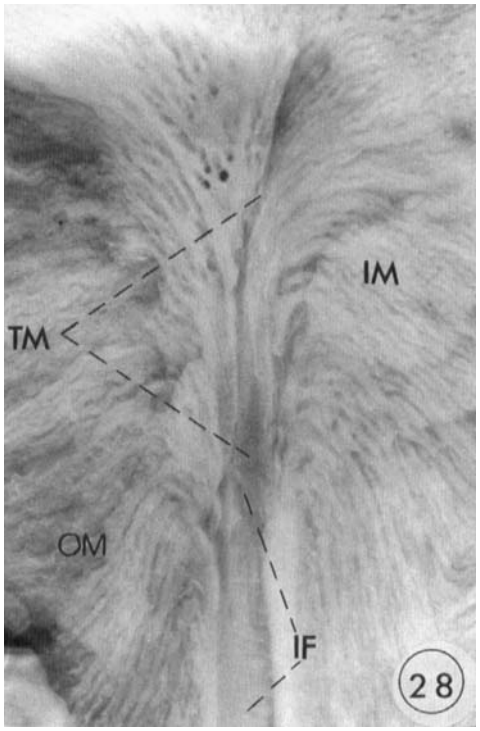

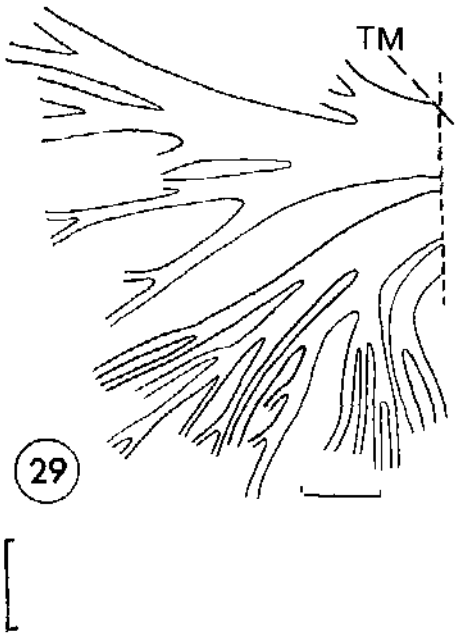

Fig. 26. Photograph of longitudinal cut, immersed in 10% formalin, through a tubus maximus and peripheral end of infundibulum of a lobe of No. 17983. Bar = 3.0 mm.

Fig. 27. Photograph of tubus maximus of Figure 36 showing extent of the pale zone of the medulla. Peripheral ends of the infundibulum and calyx are evident. Bar = 3.1 mm.

Fig. 28. Photograph of longitudinal cut, immersed in 10% formalin, through tubus maximus and peripheral end of infundibulum of a lobe of No. 20317. Bar = 5.5 mm.

Fig. 29. Collecting ducts obtained by maceration of a slice through a tubus maximus of No. 20317. The broken line is the margin of the central end of the tubus. Bar = 200 μm.

TABLE 3. Data for cotrex of *D. bicornis*

Measurement or calculation	No. 17983	No. 20317
Cortex percent of kidneys	64.3	65.9
Peripheral thickness (mm)	7–11	
Thickness at interlobar septa (mm)	3.5–7	
Diameter of glomerular capsules (μm)	242.2 ± 12.4 (n = 18)	246.5 ± 12.5 (n = 18)
Volume of glomerular capsule (mm^3)	0.00742	0.007795
No. of glomeruli/gm cortex	11,144	7,071
No. of glomeruli/low-power field of cortex at ×35	15.5 ± 3.4 (n = 25)	6.9 ± 1.8 (n = 29)
No. of glomeruli in two kidneys	25.8×10^6	24.2×10^6
Mass of glomeruli (g)/kidney	98.3	101
Mass of glomeruli percent of cortex	8.24	5.90
Mass of glomeruli percent of kidney	5.30	3.89
Diameter of peripheral glomerular capsules (μm)	259.6 ± 13 (n = 6)	262.5 ± 18 (n = 6)
Diameter of midcortical glomerular capsules (μm)	234.9 ± 11.2 (n = 6)	245.1 ± 10.5 (n = 6)
Diameter of juxtamedullary glomerular capsules (μm)	232.0 ± 13 (n = 6)	232.0 ± 16 (n = 6)
Diameter of glomerular capsules overall (μm)	244 ± 13 (n = 36)	

(Maluf, 1987). Although *R. unicornis* has more glomeruli per kidney, the smaller size of its glomeruli allows its fraction of glomeruli per cortical mass to approach that for *D. bicornis*.

Medulla, Including the Tubi Maximi

The kidney is 35% medulla. The cortex of a lobe envelops the corresponding medulla except at the lobar outlet around the infundibulum (Figs. 3, 4, 11–15, 20, 25, 26). The width of medulla from tubus maximus to corticomedullary border is 17 ± 6 mm (Table 4; Figs. 22–24, 26–28). The range is from 10 mm (Fig. 15) to 42 mm (Fig. 14). The ratio of thickness of cortex to medulla averages 4.2/17 or 0.25.

In the center of the medulla is a pale zone, which corresponds roughly to the inner medulla. It extends 6–12 mm peripheral to its tubus maximus (Figs. 22–24, 26–28). The inner medulla includes the bifurcating collecting ducts, 61–87 μm in outer diameter (o.d.), an ample interstitium, the tubus maximus, the thin medullary loops, and dispersion of the vasa recta. The terminal collecting ducts open along the tubus maximus (Figs. 11–15, 20, 22–24, 26–29). The outer diameter of these ducts, the wall of which is columnar epithelium, is 204 ± 88 μm (n = 7). The length of a tubus maximus is from 5 to 30 mm and is shortest where two tubi come together within a broad lobe (Fig. 14). The lumen of a tubus is about 1 mm wide and nearly equals that of the infundibular apex of which it is an extension.

Deep to 4 mm from the corticomedullary (C-M) border, the thick tubules, 54–61 μm o.d., straighten from their sinuous course. At various depths from the C-M border, but within the outer medulla, the thick descending tubules taper gradually to thin segments with 15.2–17.4 μm o.d. In the outer medulla, deep to 7 mm from the C-M border and throughout the outer medulla, there are thick medullary loops (of Henle) about 31 μm o.d. The limbs of a loop average 35 μm apart. Thin medullary loops, a continuation of the thin segments, occur throughout the pale zone to within 200 μm of the tubus maximus. The limbs of the thin loops are 35.2 ± 26.3 μm (n = 10) apart. Thin loops occur as far as 10–20 mm from the tubus maximus apparently depending on the extent of the pale zone. No estimate was made of the ratio of thick and thin loops. The impression is that the thin loops dominate.

Arteries

A hitherto unreported feature is the manner by which all branches of the renal artery of rhinoceri enter the renal substance. In *D. bicornis*, the outer diameter of the renal artery is 20 mm, and its wall thickness is about 1.5 mm. The renal artery enters the hilum dorsal to the renal vein (Figs. 1b, 34). It divides promptly into branches 3.5–6 mm in outer diameter. The primary, secondary, tertiary, and quaternary branches at the hilum and within the renal sinus enter the renal substance mostly through the interlobar septa (Figs. 20, 27–39) with an average initial outer diameter of 2.27 ± 1.46 mm (n = 20). These interlobar arteries branch within their septa (Figs. 40, 41) and thence give off perforating arteries into the adjacent cortex. This can be shown by scooping out cortex and medulla with a fine forceps under the dissecting microscope, exposing the cortical surface of the septa (Figs. 36, 37, 40, 41).

Numerous branches of the interlobar arteries perforate the interlobar septa and thus enter the cortices of adjacent lobes (Figs. 20, 35–37, 40, 41). In so doing, these perforating arteries, which are 0.8–2.5 mm in outer diameter, carry a portion of the septum with them. Upon reaching the C-M border, they branch and extend as arcuate arteries, usually superficial to the arcuate veins (Figs. 20, 30, 35, 42, 43) and supply recurrent radial or interlobular branches to the cortex. The interlobular arteries are 34 ± 22.4 μm (n = 9) across their media, which consists of two or three layers of circular muscle. Some of these arteries perforate the renal capsule to the exterior (Figs. 5–10). Interlobar arteries may, also, after branching, extend through the interlobar sulci to the exterior (Fig. 41).

In affording inward passage to an interlobar artery,

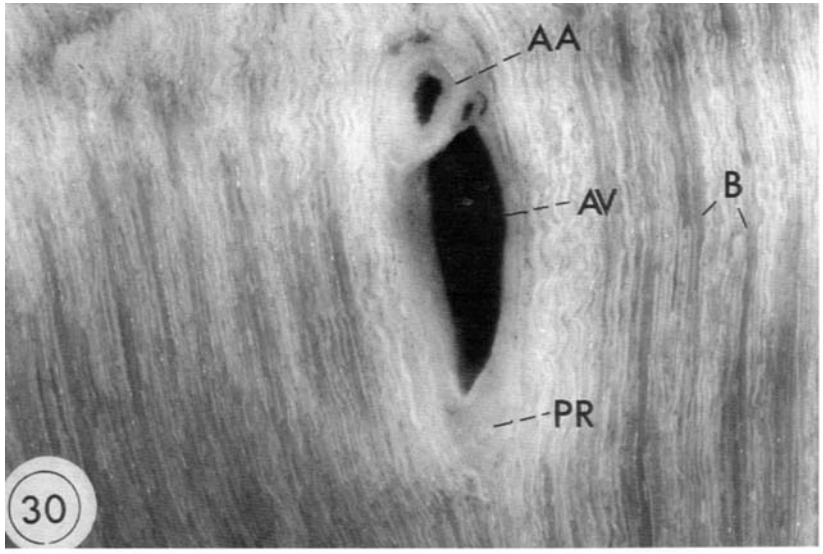

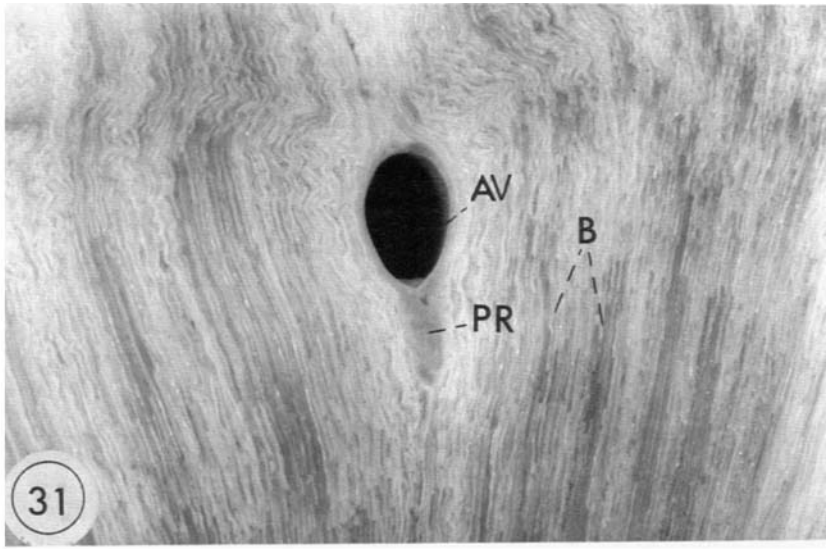

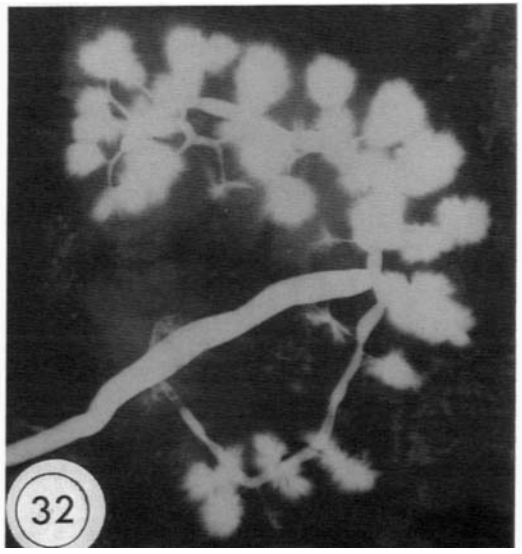

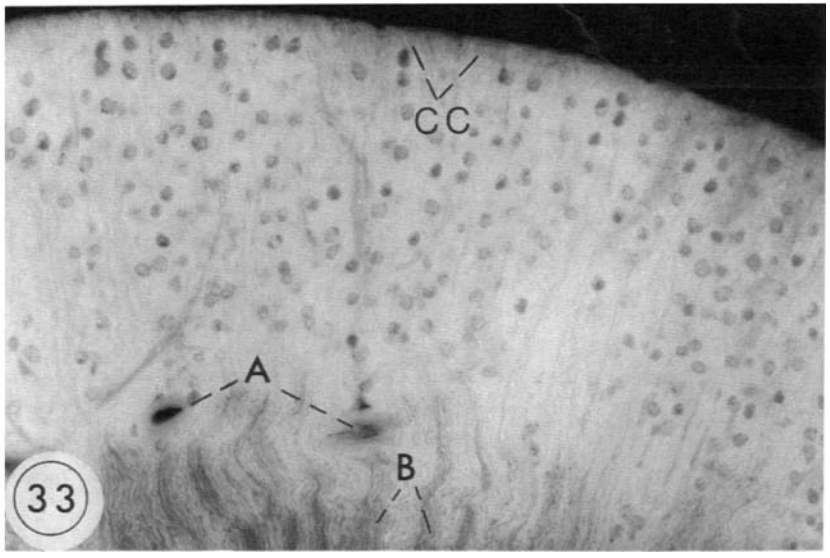

Fig. 30. Cross section through arcuate vessels near periphery of outer medulla of No. 17983. The arcuate vein is deep to the arcuate artery and has a thickening on the medullary side as a projection, which is made of collagen and muscle fibers also in cross section. Fixed tissue immersed in 10% formalin. Bar = 1.2 mm.

Fig. 31. Cross section through an arcuate vein of No. 20317 not associated with an arcuate artery. The central wall of the vein projects into the medulla. Fixed tissue immersed in 10% formalin. Bar = 1.2 mm.

Fig. 32. Retrograde pyelogram of left kidney of No. 20317. The opaque fluid has entered terminal collecting ducts giving a bushy appearance. Some of the infundibula of the caudal conduit are not filled. Bar = 50 mm.

Fig. 33. Cut through cortex of No. 17983. There is a defined cortex corticis (cc) and the glomeruli are the same size throughout the cortex. Fixed tissue immersed in 10% formalin. Bar = 2.5 mm.

TABLE 4. Data for medulla of *D. bicornis*

Percent of renal mass, No. 17983	35.7
Percent of renal mass, No. 20317	34.1
Width (mm)	17 ± 6 (range 10–42)
Ratio of widths, cortex/medulla	0.25
Width of pale zone (mm)	6–11
Terminal collecting ducts, outer diameter (μm)	204 ± 88 (n = 6)
Length of tubus maximus (mm)	5–30
Lumen of tubus maximus, diameter (mm)	1.0
Thin loops, diameter (μm)	15–17
Distance between limbs of a thin loop (μm)	35.2 ± 26.3 (n = 10)
Distance from cortico medullary border at which tubules taper down (mm)	15–17
Distance of thin loops from tubus (μm)	200–10,000
Thickness of vascular bundles (μm)	60–113
Distance apart of vascular bundles at 3 mm from corticomedullary border (μm)	500–1,200

the interlobar septum splits so that the interstitium between artery and septum is filled with areolar fascia, nerves, capillaries, and small veins (Figs. 38, 39). In absence of an interlobar artery the septum is sealed and thus helps maintain rigidity of the kidney. Other branches of the renal artery, about 1.5 mm in outer diamter, enter the cortex directly, carrying renal capsule with them, and form arcuate branches at the C-M border as do those that perforate via the interlobar septa.

Branches of the renal artery proceed similarly in the three rhinoceri: *D. bicornis*, *R. unicornis*, and *C. simum*. In short, they enter the kidney in two ways: 1) through the interlobar septa and 2) in a lesser manner, directly through the cortex from the exterior.

Veins

Arcuate veins (Fig. 35) form an anastomotic network between cortex and medulla. They are of variable width (1,353 ± 817 μm; n = 14), are usually central to an associated artery (Fig. 46), and tend to be indented by the artery (e.g., Fig. 30). The wall of these veins that contacts the cortex typically consists of endothelium only. On their medullary surface, however, the endothelium is enforced by a thick fibromuscular scaffolding (Figs. 30, 31) containing small blood vessels and projecting 400–1,000 μm into the medulla (Fig. 46). The muscular and collagenous fibers of the scaffolding run parallel with and central to the arcuate veins. In Figure 46, the arcuate veins, artery, and scaffolding are in cross section. In Figure 47, part of the scaffolding is further enlarged, showing cross sections of the muscular (dark) and collagenous (lighter) fibers. The walls of the interlobular veins, which average 114 ± 51 μm (n = 10) in diameter, consist of endothelium only, and they tend to hug the contours of the adjacent convoluted tubules. This is true also in rat, rabbit, and man (Dietrich, 1978; Jamison and Kriz, 1982). The writer finds that this applies to the following mammals: these three species of rhinoceros, horse, tapir, manatee, African elephant, juvenile and adult okapi, juvenile and adult Masai giraffe, hippopotamus, ox, domestic pig, cat, and dog (unpublished). Since no exceptions have been found, this may hold for the interlobular veins of mammals generally.

A conspicuous feature of the venous system, as in *R. unicornis* (Maluf, 1987), is the large intralobar veins (Figs. 20, 22–24, 26, 36), which course between cortex and medulla at the central end of every lobe. These veins are 1,761 ± 1,019 μm (n = 23) in diameter and receive arcuate veins through prominent valved orifices (Figs. 20, 36). From the C-M border, an intralobar vein may traverse the outer medulla without tributaries (Fig. 45). In its course toward becoming interlobar, the intralobar vein establishes contact with calyx, outer medulla, and renal capsule (Fig. 20, 36). Areolar fascia separates the intralobar veins from the associated infundibulum, but these veins are securely fused to outer medulla and to renal capsule. The interlobar veins are 5–9 mm wide and course within the areolar fascia between pelvic conduits and renal capsule. They join, via valved orifices, a major vein that runs alongside the pelvic conduits.

The single left renal vein, 40 mm in diameter with a wall about 1 mm thick, spreads across the ventral surface of the hilum (Figs. 1b, 34). At the posterior vena cava, its ostium is supplied with a translucent valve. This is 28 mm wide, 30 mm deep, and at its free margin 174 μm thick. It consists of collagen and elastin. The valved ostium of the right renal vein is similar and is 2.5 cm cephalad of the left. The vena cava at the level of the ostia is 37 mm in diameter with a wall 3 mm thick. The latter consists of longitudinal bundles of smooth muscle interspersed with collagen (Fig. 18). Surrounding the muscle fibers are numerous longitudinal fibrils of elastin (Fig. 19).

Renal Capsule and Interlobar Septa

The cortical surface is covered by the renal capsule, which is fixed to and is part of the interlobar septa. The capsule is a tough, fibromuscular,[1] semitranslucent membrane which is 140–384 μm thick. Its muscle fibers, which stain red conspicuously with Masson's trichrome (Fig. 48) and light yellow with Weigert's or Verhoeff's, are in the deeper third of the capsule and extend into the interlobar septa (Figs. 20, 50). The collagen bundles, which are blue with the trichrome and light pink with the elastin, are intermingled with the muscle but are also superficial and extend into the core of the interlobar septa. Elastic fibers follow the course of the collagen bundles at the periphery. The capsule extends into the renal sinus, where it is fixed to the intralobar veins (Figs. 20, 36). The renal capsule and the renal septa contain small blood vessels. The writer has doubted the existence of muscle fibers in the capsule of *R. unicornis* (Maluf, 1987; compare Fig. 49 for *R. unicornis* with Fig. 50 for *D. bicornis*).

The interlobar septa occur only between cortices of adjacent lobes (Fig. 21), are 170–260 μm thick, and are interrupted randomly as in *R. unicornis*. Since the interlobar septa (Fig. 20) are extensions of the renal cap-

[1]James T. McMahon, PhD, electron microscopist at the Cleveland Clinic, has confirmed, by electron microscopy, the presence of smooth muscle cells in renal capsule and interlobar septa of these rhinoceri.

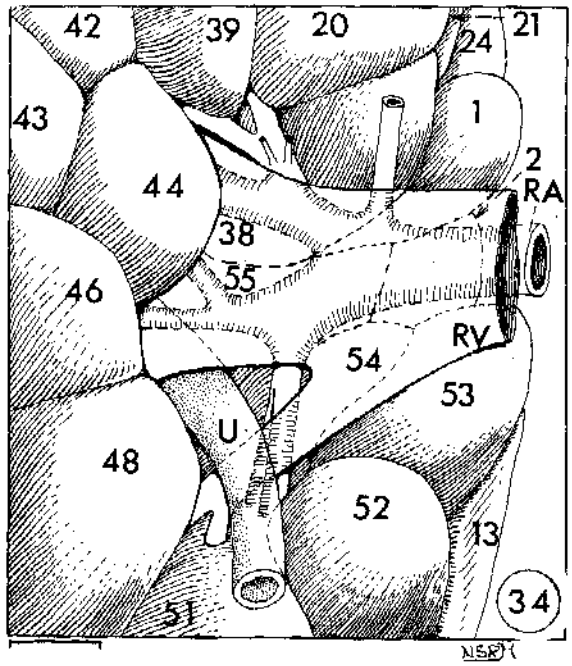

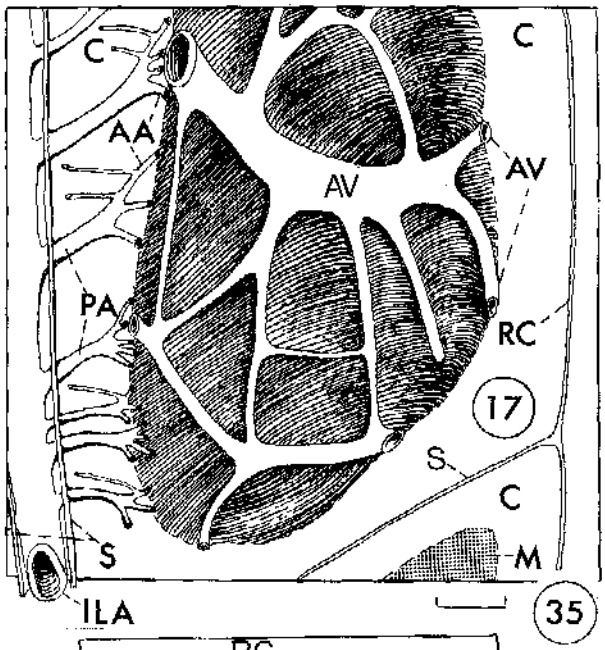

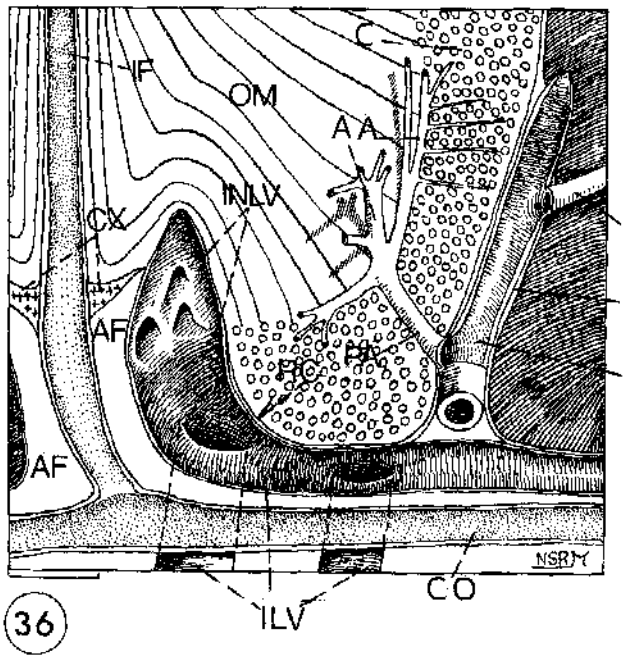

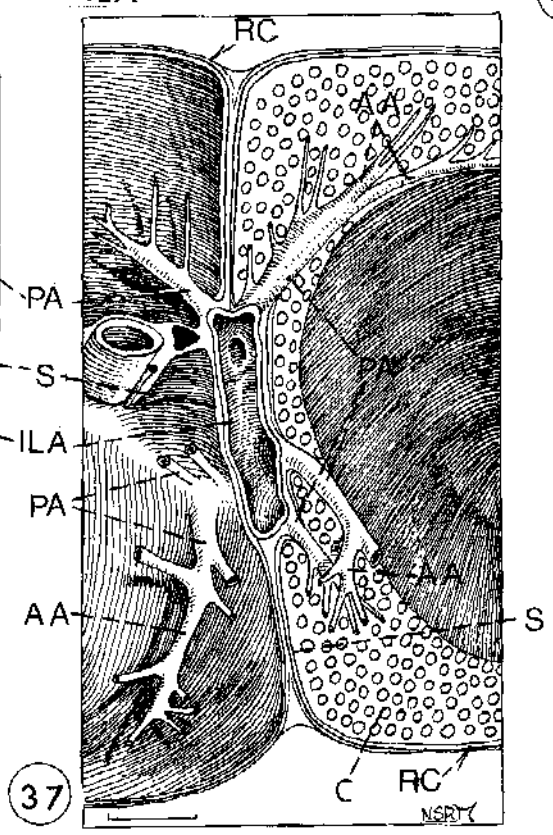

Fig. 34. Hilar structures of right kidney of No. 17983. The perihilar lobes are spread apart. Bar = 22.9 mm.

Fig. 35. Section through a lobe of No. 20317 from which the medulla (M) has been scooped out exposing a corticomedullary surface (shaded) with anastomosing arcuate veins. The adjacent interlobar artery, within the interlobar septum, has been exposed together with its branches, namely, the internal perforating arteries, which extend to the corticomedullary border and become arcuate arteries. Tributaries to the arcuate veins are not shown. Bar = 6 mm.

Fig. 36. Longitudinal section through part of base of a lobe of No. 20317, showing interlobar artery within interlobar septum, internal perforating artery, large intralobar vein, infundibulum, and pelvic conduit. The cortex has been scooped out of the partial lobe at the right. Bar = 2.4 mm.

Fig. 37. Cross section through part of two lobes of No. 17983 showing interlobar artery, within interlobar septum, and internal perforating arteries. The cortex and medulla have been scooped out of the lobe at the left showing perforating arteries emerging through the interlobar septum. The medulla has been scooped out of the lobe at the right showing internal perforating arteries becoming arcuate arteries. Bar = 2.4 mm.

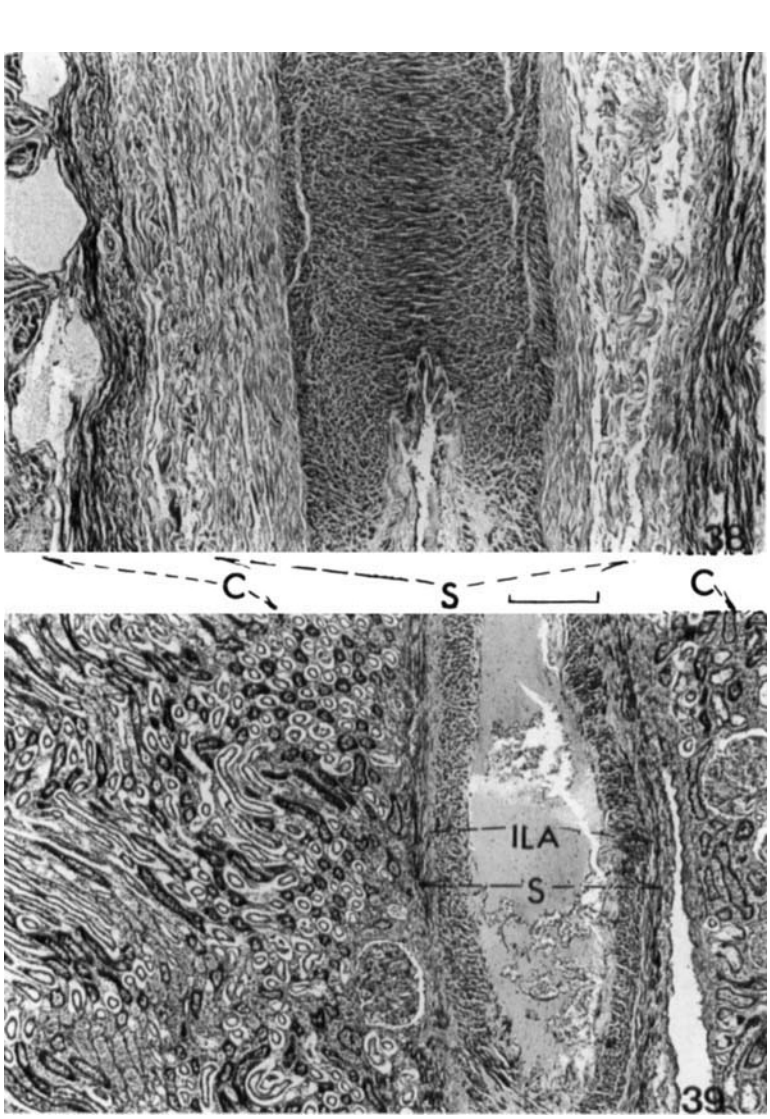

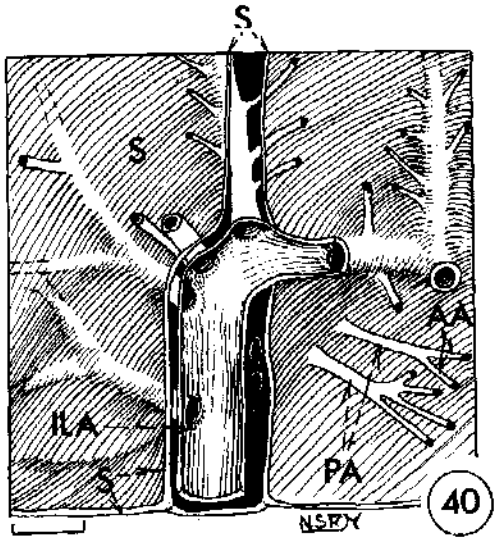

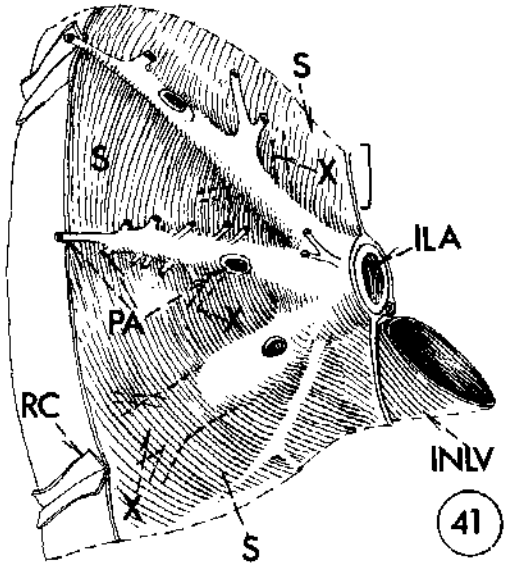

Fig. 38. Photomicrograph of longitudinal section through an interlobar artery enclosed within its interlobar septum. No. 17983. Masson's trichrome; Kodak green filter 58. Bar = 158 μm.

Fig. 39. Photomicrograph of longitudinal section through an interlobar artery enclosed by its interlobar septum. The cortices of adjacent lobes are on each side of the septum. No. 17983. Masson's trichrome; Kodak green filter 58. Bar = 193 μm.

Fig. 40. Dissection of an interlobar artery, showing its branching within the interlobar septum, and the internal perforating arteries which enter the respective cortices and gain the cortico medullary borders as arcuate arteries. No. 17983. Bar = 4.3 mm.

Fig. 41. Dissection of an interlobar artery, showing its branching within the interlobar septum. The branches (in broken lines, *X*) enter another interlobar septum, which connects with the first septum. Many internal perforating arteries enter the respective cortices and gain the corticomedullary borders as arcuate arteries. No. 17983. Bar 3.5 mm.

sule, they cannot actually reach the pelvic conduits. Between renal capsule and conduits is areolar fascia containing blood vessels and nerves.

DISCUSSION

Kidney of Rhinocerotidae: Comparative

In the Rhinocerotidae, the renal pelvis is extended as a fibromuscular conduit, cephalically and caudally, from which fibromuscular infundibula proceed transversely in all directions and communicate individually with the many closely packed, circumscribed lobes via a large common collecting duct, or tubus maximus supplied to every lobe. The renal pelvis of their perissodactyl relatives, the Equidae or horses, is small but is extended cephalically and caudally into a relatively wide tubus maximus. The equid kindey has no lobes and no branching of the tubus. The terminal collecting

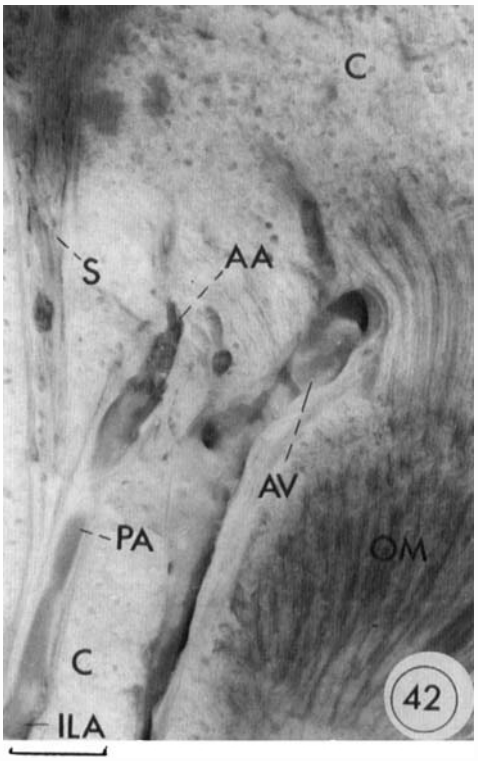

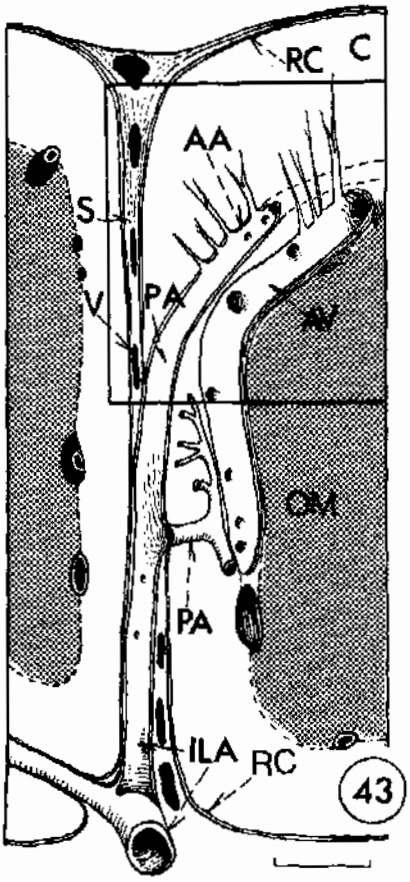

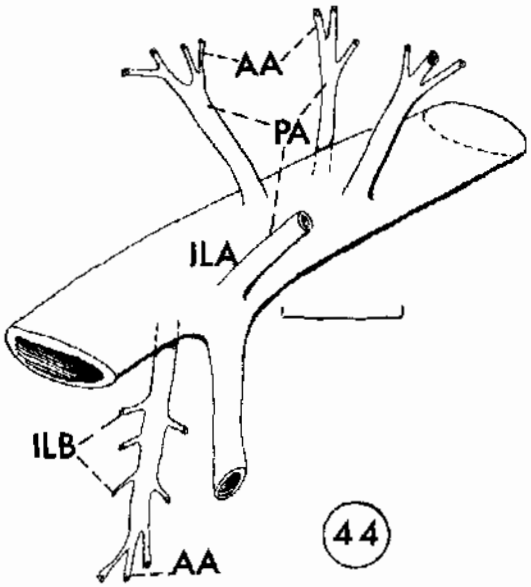

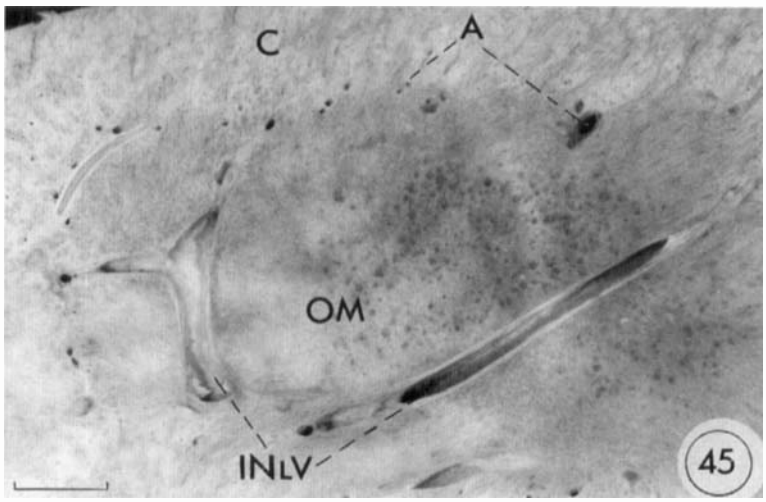

Fig. 42. Photograph of cut, immersed in 10% formalin, through interlobar septum and adjacent lobes. An interlobar artery perforates the septum as a perforating artery and extends across the cortex to become an arcuate artery. The arcuate vein is subjacent. No. 17983. Bar = 3.5 mm.

Fig. 43. An interlobar artery perforates an interlobar septum and extends across the cortex to become an arcuate artery. Structures within the rectangle are photographed in Figure 28.

Fig. 44. Isolated interlobar artery showing internal perforators (PA), which enter three adjacent lobes and extend to the respective corticomedullary borders becoming arcuate arteries. In their course through the cortices they give off interlobular arteries (ILB). No. 20317. Bar = 6.5 mm.

Fig. 45. Photograph of cut, immersed in 10% formalin, through a lobe of No. 20317 showing intralobar veins coursing through outer medulla from the corticomedullary border. They receive no tributaries in their passage through the medulla. Bar = 3.5 mm.

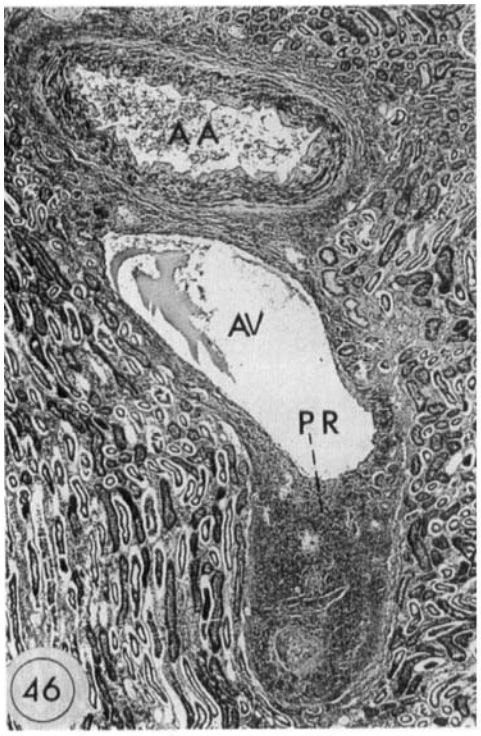

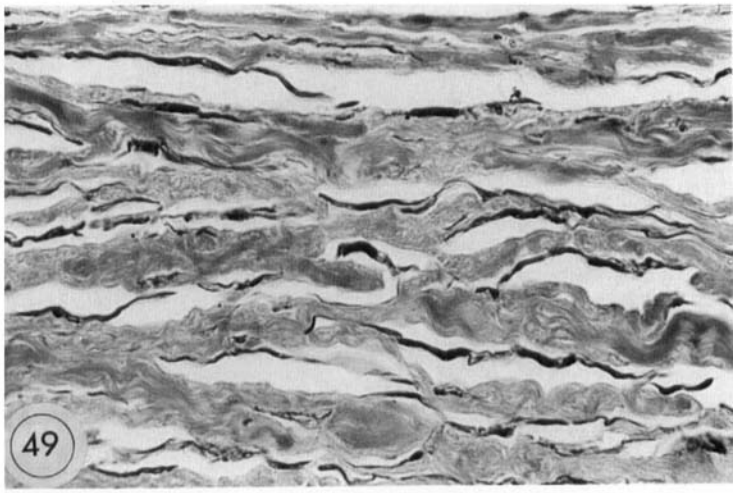

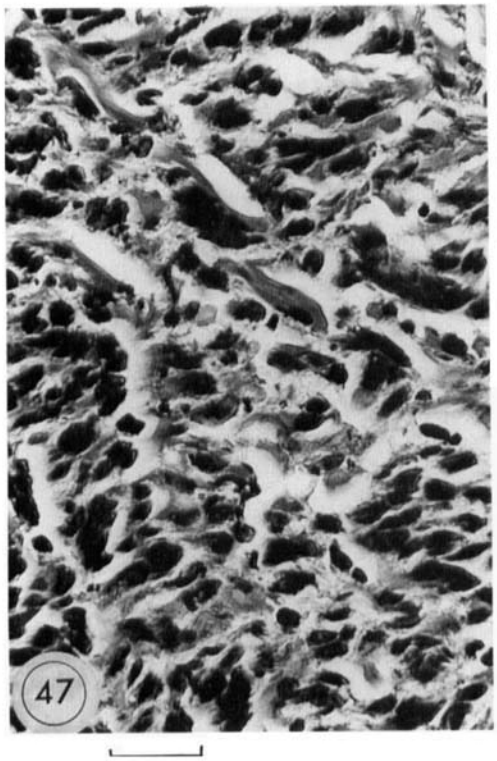

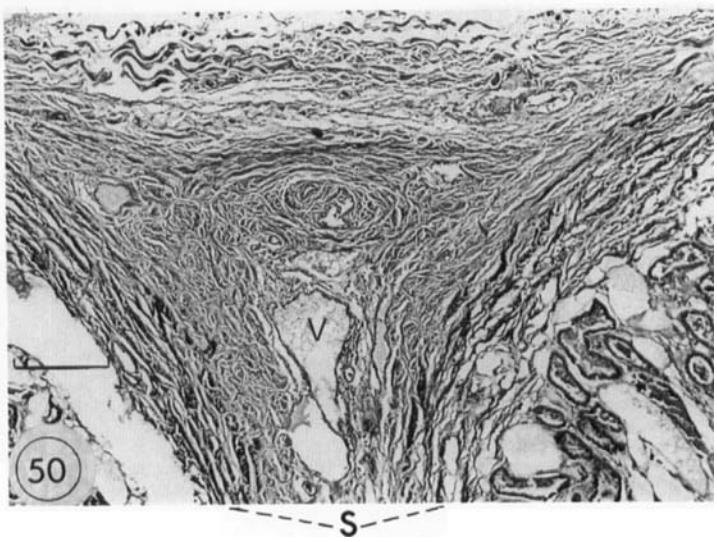

Figs. 46–50.

ducts (of Bellini) open all along the tubus, which they would not be able to do with a fibromuscular conduit.

Closest to the rhinoceros kidney is apparently that of the Hippopotamidae. Here the pelvis is diminutive and extends cephalically and caudally into a relatively narrow tubus maximus. The hippopotamus kidney is lobed transversely, and the main tubus gives off a secondary tubus maximus to every lobe (Maluf, 1978, and unpublished data). The hippos are classed as artiodactyls (Simpson, 1945; Colbert, 1969). Their kidney, however, is unlike that of any other known artiodactyl.

Transverse Lobation

Toldt (1874) appears to have been the first to write that during human fetal development the rencules [lobes] generally are arranged so that there are three or four anteriorly and the same number posteriorly with a deep furrow between them along the lateral border. Felix (1912) reported "horizontal dorsal and ventral primary tubules" extending from the renal pelvis of human embryos. Ludwig (1962) presented similar data. Löfgren (1949) described transverse lobation in fetal and neonatal human embryos. Heidenhain (1937) noted girdle-like transverse segmentation of the kidney in advanced fetuses of ox and man. Hill (1945) described dorsal and ventral extensions of the renal pelvis of the dugong forming a girdle suggesting transverse lobation. Von Kügelgen et al. (1959) observed transverse lobation in the canine kidney, which has a medullary crest. Maluf (1981) described transverse lobation in the kidneys of okapi and giraffe, which have a medullary crest, and noted that the interlobar vessels course dorsally and ventrally along the projectio vascularis pelvina (extensions of the pelvic cavity along the interlobar vessels), even when lobes are not clearly defined externally.

The pelvic conduits of the rhinoceros are probably homologous with a bifurcating pelvis, along which lobes are arranged transversely. The infundibula are transverse extensions of the pelvis to the individual lobes. The calyces may be represented by the circular vascular bundles near the apices of the infundibula (Figs. 20, 22, 23, 26, 27). This is more obvious in *R. unicornis*, in which the fibromuscular calyces intrude between cortex and medulla and are intimately attached to the intralobar veins (Maluf, 1987).

Tubus Maximus

Hyrtl (1870, 1872) wrote that there is only one method by which the anatomical relations of the renal pelvis can be ascertained and that is by corrosion after a mass has been injected into the pelvis via the ureter. After using the method for the kidney of an African elephant, he reported a helical proximal ureter and papillary impressions (Warzeneindrücke) at the end of long funnel-shaped calyces. "At the two most anterior calyces the tubuli belliniani of the corresponding medulla unite into a single short tubus maximus" (Hyrtl). He reported no histological observations and used tubus maximus only once, and this in the legend for that kidney (his plate II, Fig. 1). Although he had an excellent cast of the equine pelvis and its extensions (his Fig. 2, mislabelled Fig. 3 in his legends), now known as standard examples of tubi maximi, he did not name them thus, but rather "anterior and posterior extensions of the pelvis fully surrounded by numerous tubules of Bellini."

In the elephant, the terminal collecting ducts typically open at a short blunt papilla (Perrault, 1734; Mayer, 1847; Hunter, 1861; Cuvier and Duvernoy, 1840; Owen, 1868; Miall and Greenwood, 1878, 1879; Paterson and Dun, 1898; Sperber, 1944; Maluf, 1989b). Variations probably occur so that the area cibrosa may be flat (Camper, 1802; Pettit, 1907 or concave (Watson, 1873; Schulte, 1937) or there may be small tubi maximi (Sperber, 1944). Plateau and Liénard (1881) admittedly studied a hypotrophic kidney. Grahame (1944) and Dönitz (1872) studied casts and denied papillae.

Although tubi maximi may not be typical in elephants, for which the name originated, the term is useful when applied to a supreme collecting duct lined by collecting duct epithelium, with no definitive wall and into which terminal collecting ducts open around. Thus the term is applicable to the cephalic and caudal extensions of the diminutive renal pelvis of the Equidae and Hippopotamidae, to the lobar branches of these extensions in the Hippopotamidae, and to the receptacles of the terminal collecting ducts in every lobe of the Rhinocerotidae.

A plausible assumption is that no appreciable exchange of water or solutes occurs between the urothelial-lined pelvic conduits and infundibula and the renal substance. Hence, in the rhinoceri, horses, and hippopotami, the only portion of the kidney that may come into effective exchange with the definitive urine is the tubus maximus, which is part of the inner medulla.

Arteries: Comparative

During investigation of the arterial system of the *Diceros* kidney, new findings have emerged that apply also to the kidneys of the African broad-lipped or "white" rhino, *Ceratotherium simum*, Burchell, and to those of the Asiatic *Rhinoceros unicornis*. The single renal artery splays abruptly at the hilum and within the renal sinus into primary, secondary, tertiary, and even quaternary branches. Most of these branches enter the kidney through its interlobar septa, where they branch further and thence supply numerous perfora-

Fig. 46. Photomicrograph of cross section through an arcuate artery and vein of No. 17983 showing the fibromuscular process underlying the vein. Masson's trichrome; Kodak green filter 58. Bar = 300 μm.

Fig. 47. Cross section through part of fibromuscular process of Figure 40. The black patches are muscle; the gray are collagen; interstices are white. Masson's trichrome; Kodak 58 green filter. Bar = 14 μm.

Fig. 48. Section through renal capsule of No. 17983. The black bands are muscle; the gray are collagen; interstices are white. Masson's trichrome; Kodak 58 green filter. Bar = 14 μm.

Fig. 49. Section through renal capsule of *R. unicornis*, No. 21824. The black strips are allegedly muscle; the gray are collagen; interstices are white. Masson's trichrome; Kodak 58 green filter. Bar = 14 μm.

Fig. 50. Cross-section through an interlobar sulcus of No. 20317. Muscle fibers (black) dominate in deep layer of renal capsule and at periphery of interlobar septum. Collagen fibers (gray) dominate in peripheral layer of renal capsule and in interior of septum. Masson's trichrome; Kodak 58 green filter. Bar = 170 μm.

tors to the corresponding cortices. Since the cortices of three lobes are juxtaposed (Fig. 21), a single such interlobar artery can supply all three lobes (Fig. 44). The other route of arterial supply is directly through the cortex from without. Upon arrival at the C-M border, these arteries branch into arcuate vessels, which give out interlobular arteries toward the periphery. Anomalous or polar arteries to the human kidney, often incorrectly termed *accessory*, behave similarly.

In another perissodactyl, the horse, the renal artery divides abruptly at the hilum into primary to quaternary branches. These enter the cortex directly at the hilum and, variably, across the entire ventral surface of the kidney, even as far as the lateral border. As in the rhinoceri, the equine kidney is quasi-C-shaped but has no interlobar septa. Thus, in the horse, most of the branches of the renal artery enter the cortex directly from without. These perforating arteries are accompanied by the renal capsule to the C-M border without giving branches to the cortex en route. By selective injection of branches of the renal artery, the writer finds that every branch supplies its own renal segment, there being no arterial anastomoses (unpublished data).

The only known mammals, other than the rhinoceri, in which most of the major branches of the renal artery pass through the interlobar septa are the Hippopotamidae, *Choeropsis liberiensis* (Maluf, 1978) and *Hippopotamus amphibius* (unpublished data). These are, paradoxically, artiodactyls. As in rhinoceros and horse, the renal artery splays at the hilum into 2, 3, and 4 branchings. Most branches enter the interlobar septa, whereas the others enter the cortex directly. As in the rhinoceri, numerous branches of the interlobar arteries perforate the interlobar septa and thence enter directly the adjacent cortices. Herodotus (ca. 500 to 424 BC), an Ionian, gave the hippopotamus its name (Greek for river horse) after his travels up the Nile. Linnaeus (1735) called it *Equus marinus* and placed it next to the horses, asses, and zebras, as a member of the Jumenta or beasts of burden. These citations serve to accentuate the unique position of the hippo kidney among the artiodactyls.

Fibromuscular Scaffolding

Krause (1842) observed that the kidney is "harder, firmer, and more compact than all other glands." This is true even after the kidney has been bled out and decapsulated. That intertubular fibrils of collagen (Kolster, 1910; Becker, 1968; Hamburger et al., 1971) contribute to renal integrity becomes evident when a slice of kidney is temporarily subjected to collagenase or to concentrated hydrochloric acid.

Narath (1940, 1951) described musculi levatores fornices, which are fibromuscular fascicles extending from the apex of the calyceal fornix to connective tissue at the C-M border directly deep to the arcuate vessels. Comparison of Figure 1 of Narath (1940) with Figure 1 of Jardet (1886) suggests identity of Jardet's fibres musculaires divergentes with Narath's m. lev. fornices. By use of Masson's trichrome, the writer has confirmed the m. lev. fornices in man and dog. In the African elephant, these fibromuscular structures are striking (Maluf, 1989b).

Doležel (1957, 1975) noted, in various mammals, that the fibromuscular extensions of the calyx run directly deep to, but separately from, the arcuate vessels, forming a network at the C-M border. Jardet (1886) had observed, in the human kidney, fibromuscular fascicles "which divide as do the [arcuate] vessels," forming a network (réseau) at the C-M border. Such fibromuscular structures are clearly evident in the rhinos *D. bicornis* (Figs. 30, 31, 46, 47) and *C. simum* (neonate and adult), but less so in *R. unicornis*. They are distinct in cats, dogs, sloth-bears, oxen, and bison (unpublished data). In dogs, at least, they are supplied with adrenergic nerve fibers (McKenna and Angelakos, 1968).

An exaggerated fibromuscular network along the C-M border central to the arcuate vessels, and extending from the calyx of every renculus, occurs in Cetacea including river porpoises (Cave and Aumonier, 1961, 1984; Cave, 1973, 1977). This sportella (small basket) is readily distinguishable from adjacent arcuate vessels. In the adult finback whale, *Balaeonoptera physalis* L., and sperm whale, *Physter macrocephalus* L., it is chiefly collagenous (unpublished data).

ACKNOWLEDGMENTS

At Case Western University School of Medicine, Stephen D. Sindely made the histological sections, Michael D. Thomas and Ken I. Kondo took the photographs. The pyelogram (Fig. 32) was taken by Mrs. Clara Adair in the office of Anthony W. Orlandella, MD, South Laguna, CA. The rhino and hippo kidneys were courtesy of Dr. Marilyn P. Anderson, pathologist with the San Diego Zoological Society. *D. bicornis* No. 21362 (a third rhino incidentally included in Fig. 23) was diagnosed as having had hyperparathyroidism by Dr. Linda Munson while she was a fellow in pathology at the San Diego Zoological Society.

LITERATURE CITED

Alexander, B. 1908 From the Niger to the Nile. Edward Arnold, London.

Asdell, S.A. 1946 Patterns of Mammalian Reproduction. Comstock Publ., Ithaca, NY.

Baer, P.G., G. Bianchi, and D. Liliana 1978. Renal micropuncture study of normotensive rats before and after development of hypertension. Kidney Int, *13*:452–466.

Baker, S.W. 1868 The Nile Tributaries of Abyssinia. Lippincott, Philadelphia.

Barber, W. 1958 Surgery and the Mau Mau. J. R. Army Med. Corps, *104*:41–43.

Becker, E.L., ed. 1968 Structural Basis of Renal Disease. Harper & Row, New York.

Bruce, J. 1791 Travels to Discover the Source of the Nile in the Years 1768 to 1773, Vol. 5. Graisberry & Campbell, Dublin.

Camper, P. 1802 Déscription Anatomique d'un Éléphant Mâle. H.J. Jansen, Paris.

Cave, A.J.E. 1973 Observations on the renal morphology of the Indian river dolphin (*Platanista indi*). Invest. Cetacea, *5*:71–81.

Cave, A.J.E. 1977 The reniculus in *Hyperoödon* and *Orcinus*. Invest. Cetacea, *8*:103–121.

Cave, A.J.E., and F.J. Aumonier 1961 The visceral histology of the primitive cetacean *Caperea (Neobalaena)*. J. R. Microsc. Soc., *80*: 25–33.

Cave, A.J.E., and F.J. Aumonier 1964 The reniculus in certain balaenopterids. J. R. Microsc. Soc., *83*:255–264.

Chaplin, H., A.C. Melecek, R.E. Miller, C.E. Bell, L.S. Gray, and V.L. Hunter 1986 Acute intravascular hemolytic anemia in the black rhinoceros: Hematologic and immuno-hematologic observations. Am. J. Vet. Res. *47*:1313–1320.

Colbert, E.H. 1969 Evolution of the Vertebrates, 2nd ed. Wiley & Sons, New York.

Cuvier, G. and G.L. Duvernoy 1840 Leçons d'Anatomie Comparée de Georges Cuvier, 2nd ed., Vol. 7. Fortin, Masson & Cie, Paris.

Dieterich, H.J. 1978 Die Struktur der Blutgefässe in der Rattenniere. Georg Thieme Verlag, Stuttgart.
Doležel, S. 1957 The structure of renal connective tissue in the dog and its relationship to the renal vessels and nerve fibers. Ceskoslovenska Morf., 5:16–20. (In Czech with Russian and German summaries; Engish summary in Biol. Abstracts, Vol. 53; No. 6950, 1960).
Doležel, S. 1975 The connective tissue skeleton in the mammalian kidney and its innervation. Acta Anat., *93*:194–209.
Dönitz, W. 1872 Ueber die Nieren des afrikanischen Elephantin. Arch. Anat. Physiol. Wiss. Med., *85*:85–89.
Felix, W. 1912 The development of the urogenital organs. In: Manual of Human Embryology, Vol. 2. F. Keibel and F.P. Mall, eds. J.B. Lippincott Co., Philadelphia. pp. 752–979.
Gessi, R. 1892 Seven Years in the Soudan. Sampson Low, Marston & Co., London.
Grahame, T. 1944 The kidney of the Indian elephant (*Elephas indicus*). Br. Vet. J., *100*:97–102.
Hamburger, J., G. Richet, and J.P. Grunefeld 1971 Structure and function of the kidney. Saunders, Philadelphia.
Heidenhain, M. 1937 Synthetische Morphologie der Niere des Menschen. E.J. Brill, Leiden.
Hill, W.C.O. 1945 Notes on the dissection of two dugongs. J. Mammal., *26*:153–175.
Hunter, J. 1861 Essays and Observations on Natural History, Anatomy, Physiology, Psychology, and Geology, Vol. 2. (Arranged and revised by R. Owen.) John van Voorst, London, p. 172.
Hyrtl, J. 1870 Das Nierenbecken der Säugethiere und des Menschen. Kaiserlich-Königlichen Hof- und Staatsdruckerei, Wien.
Hyrtl, J. 1872 Das Nierenbecken der Säugethiere und des Menschen. Denkschr. Akad. Wissensch., Wien, Math.-Naturw. Klasse, *31*:107–140.
Jamison, R.L., and W. Kriz 1982 Urinary Concentrating Mechanism: Structure and Function. Oxford University Press, New York.
Jardet 1886 Dans la présence dans les reins, à l'état normal et pathologique, de faisceaux de fibres musculaires lisses. Arch. Physiol. Normal Pathol, *18*:93–100.
Kolster, R. 1910 Zur Kenntnis des Stützgewebes der Nieren. Z. Urol., *4*:64–148.
Krause, C.F.T. 1842 Handbuch der menschlichen Anatomie, 2nd ed. Hahn'sche Buchhandlung, Hannover. Vol. 1, part III, pp. 485–1271.
Linnaeus, C. 1735 Systema naturae, sive regna tria naturae systematice proposita per Classes, Ordines, Genera, & Species. Theodorum Haak, Lugduni Batavorum. Facs. excerpts, 1964, B. De Graaf, Nieuwkoop.
Löfgren, F. 1949 Das Topographische System der Malpighischen Pyramiden der Menschenniere. A.B. Gleerupska Univ. Bokhandeln, Lund.
Ludwig, E. 1962 Über Frühstadien des Menschlichen Ureterbaumes. Acta Anat., *49*:168–185.
Luna, L.G., ed. 1960 Manual of Histologic Methods of the Armed Forces Institute of Pathology. 3rd ed. McGraw-Hill, New York.
McKenna, O.C., and E.T. Angelakos 1968 Adrenergic innervation of the canine kidney. Circul. Res., *22*:345–354.
Maluf, N.S.R. 1978 Anatomy of the kidneys of a newly born pigmy hippopotamus (*Choeropsis liberiensis* Morton). Z. Vet. Med., (Anat. Histol. Embryol.) 7:28–48.
Maluf, N.S.R. 1981 Kidney of a juvenile okapi, *Okapia johnstoni*. Am. J. Anat., *161*:257–279.
Maluf, N.S.R. 1987 Kidney of the great Indian rhino *Rhinoceros unicornis*, Linnaeus. Am. J. Anat., *180*:403–421.
Maluf, N.S.R. 1989a Renal anatomy of the manatee, *Trichechus manatus*, Linnaeus. Am. J. Anat., *184*:269–286.
Maluf, N.S.R. 1989b Kidney of the African elephant. Anat. Rec., *232*:74A (abstract).
Masson, P. 1929 Some histological methods; trichrome stainings and their preliminary technique. J. Technical Methods Bull. Int. Assoc. Med. Mus., No. 12, pp. 75–90.
Mayer, C. 1847 Beiträge zur Anatomie des Elephantin und der übrigen Pachydermen. Novorum Actorum Acad. Caesareae: Leopoldino-Carolinae Naturae Curiosorum, *22*:1–54.
Miall, L.C., and F. Greenwood 1878 The Anatomy of the Indian Elephant. Macmillan, London.
Miall, L.C., and F. Greenwood 1879 The Anatomy of the Indian Elephant. J. Anat. Physiol., *13*:17–50.
Miller, R.E., and W.J. Boever 1982 Fatal hemolytic anemia in the black rhinoceros: case report and a survey. J. Am. Vet. Med. Assoc., *181*:1228–1231.
Narath, P.A. 1940 The hydromechanics of the calyx renalis. J. Urol., *43*:145–176.
Narath, P.A. 1951 Renal Pelvis and Ureter. Grune & Stratton, New York.
Owen, R. 1868 On the Anatomy of Vertebrates, Vol. 3. Longmans, Green, London.
Paglia, D.E., W.N. Valentine, R.E. Miller, 1986 Acute intravascular hemolysis in the black rhinoceros: Erythrocyte enzymes and metabolic intermediates. Am. J. Vet. Res., *47*:1321–1325.
Paterson, A.M., and R.C. Dun 1898 The genito-urinary organs of the female Indian elephant. J. Anat. Physiol., *32*:582–604.
Perrault, C. 1734 Mémoires pour Servir a l'Histoire Naturelle des Animaux. Vol. 3, Part 3. Déscription Anatomique d'un Éléphant. La Compagnie des Libraires, Paris, pp. 91–156.
Pettit, A. 1907 Sur le rein de l'éléphant d'Afrique (*Elephas Loxodon africanus* Blumb.). Arch. Zool. Exp. Génér., 7:CIII–CVI.
Plateau, F., and V. Liénard 1881 Observations sur l'anatomie de l'éléphant d'Afrique *Loxodon africanus* adulte. Bull. Acad. R. Sci., Belg., *45*:250–285.
Rapp, W.L. 1837 Die Cetaceen. Zoologisch–Anatomisch dargestellt. Cottaschen J.G. Buchhandl., Stuttgart.
Schulte, T.L. 1937 The genito-urinary system of the *Elephas indicus* male. Am. J. Anat., *61*:131–157.
Scott, W.B. 1937 A History of Land Mammals in the Western Hemisphere, Revised ed. Macmillan, New York.
Sidney, J. 1965 The past and present distribution of some African ungulates. Trans. Zool. Soc. London, *30*:1–397.
Simpson, G.G. 1945 The principles of classification and a classification of mammals. Bull. Am. Mus. Nat. Hist., *85*:1–350.
Sperber, I. 1944 Studies on the mammalian kidney. Zool. Bidrag, *22*:249–432.
Toldt, C. 1874 Untersuchungen über das Wachstum der Nieren des Menschen und der Säugethiere. Sitzungsber. Kaiserl. Acad. Wissensch. Wien, Math.-Naturw. Classe III., *69*:1–27.
Verhoeff, F.H. 1908 Some new staining methods of wide applicability; Including a rapid differential stain for elastic tissue. J. Am. Med. Assoc., *50*:876–877.
Von Kügelgen, A., B. Kuhlo, W. Kuhlo, and K.J. Otto 1959 Die Gefässarchitektur der Niere. Georg Thieme, Stuttgart.
Watson, M. 1873 Contributions to the anatomy of the Indian elephant. Part II. Urinary and generative organs. J. Anat. Physiol., *7*:60–74.
Weigert, C. 1898 Ueber eine Methode zur Färbung elastischer Fasern. Centralbl. Allgem. Path. Anat., *9*:289–292.